


8-2018

Projected Trends in Climate Extremes in the Passaic River Basin Based on Bias-Corrected and Spatially Downscaled Global Climate Model Simulations

Archana Prasad
Montclair State University

Follow this and additional works at: <https://digitalcommons.montclair.edu/etd>

 Part of the [Earth Sciences Commons](#), and the [Environmental Sciences Commons](#)

Recommended Citation

Prasad, Archana, "Projected Trends in Climate Extremes in the Passaic River Basin Based on Bias-Corrected and Spatially Downscaled Global Climate Model Simulations" (2018). *Theses, Dissertations and Culminating Projects*. 185.
<https://digitalcommons.montclair.edu/etd/185>

This Thesis is brought to you for free and open access by Montclair State University Digital Commons. It has been accepted for inclusion in Theses, Dissertations and Culminating Projects by an authorized administrator of Montclair State University Digital Commons. For more information, please contact digitalcommons@montclair.edu.

Abstract

Global Climate Models (GCMs) are increasingly becoming useful tools for predicting future climatic changes. These GCMs typically employ large spatial scales while municipalities may experience varied impacts at the local level. By downscaling and bias-correcting GCM outputs, more accurate predictions concerning specific regions can be made. The Multivariate Adaptive Constructed Analogs (MACA) models provide daily precipitation and temperature information for point localities by modifying coarse resolution data from GCMs to a higher spatial resolution. In this study, trends in climate extremes over the Passaic River Basin (PRB) between 1981-2005 are estimated based on three MACA models (bcc-csm1-1m, CCSM4, and MRI-CGCM3). The historical trends obtained from the MACA models are validated using an observational dataset and further corrected for bias, and then projected trends for 2051-2075 relative to the 1981-2005 investigated.

The models are united in their expectations of a decrease in very cold nights, ranging from -0.05% to -0.25%. Warm nights show slightly less agreement; while bcc-csm1-1m and MRI-CGCM3 see an increase ranging from 0.05% to 0.18%, CCSM4 sees a decrease of 0.075% for RCP 8.5. Consecutive dry days decrease by up to 3 days between CCSM4 and MRI-CGCM3, whereas bcc-csm1-1m only shows an increase in CDD for scenario RCP 8.5. Rainy days also increase per model from 1-3 days except for bcc-csm1-1m, which sees a decrease by 1 day. The 95th percentile of (or extreme) precipitation also sees almost universal increase ranging from 25% to 80% except for MRI-CGCM3, which projects a slight decrease of the extreme at only -5%.

This analysis presents a unique opportunity to glimpse at the projected changes in the PRB with regards to the impacts of climate change.

MONTCLAIR STATE UNIVERSITY

PROJECTED TRENDS IN CLIMATE EXTREMES IN THE PASSAIC RIVER BASIN BASED ON
BIAS-CORRECTED AND SPATIALLY DOWNSCALED GLOBAL CLIMATE MODEL
SIMULATIONS

by

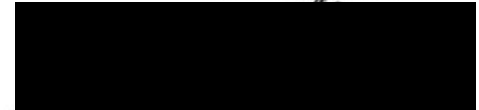
Archana Prasad

A Master's Thesis Submitted to the Faculty of Montclair State University
In Partial Fulfillment of the Requirements for the Degree of
Master of Science

August 2018

College of Science and Mathematics
Department of Earth and Environmental Studies

Thesis Committee:



Dr. Clement A. Alo
Thesis Chair



Dr. Robert W. Taylor
Committee Member



Dr. Joshua C. Galster
Committee Member

Projected Trends in Climate Extremes in the Passaic River Basin Based on Bias-corrected and
Spatially Downscaled Global Climate Model Simulations

A THESIS

Submitted in partial fulfillment of the requirements
for the degree of Master of Science

by

ARCHANA PRASAD

Montclair State University

Montclair, NJ

2018

Copyright © 2018 by Archana Prasad. All rights reserved.

Acknowledgments

Firstly, I would like to thank Dr. Clement Alo for his guidance for the duration of this thesis. Through the successes and missteps, you have consistently believed in my capacity for science. The dignity and respect you afforded me provided the best motivation to power through the research obstacles.

I am also appreciative of my committee members, Dr. Josh Galster and Dr. Robert Taylor. To Dr. Galster: thank you for your approachability, your availability, and helpfulness in ensuring I maintained a reasonable timeline. Dr. Taylor: thank you for your encouragement and sharing your knowledge of sustainable development, which has helped me navigate a path for myself.

My heartfelt gratitude to my friends and family, without whose kindness I could not have completed this thesis. This especially extends to my sister and part-time guru, Dr. Bidya Prasad-de Vreede, whose constant willingness to guide and help me through even the worst moods kept me afloat; to my younger brother turned older, Rohit Prasad, whose humor kept me laughing; to the Gayle to my Oprah, Mira Patel, whose graciousness and sense of adventure inspired me; to Felix Oteng, whose patience in providing countless hours of mentoring and technical help have never gone unappreciated; and to Taylor Wiczerak, Dr. Bernabas Wolde, Dr. Pralhad Burli, and Dan Ciarletta for never hesitating to provide help or insight.

I would like to dedicate this thesis to my parents, Ramanuj and Anita Prasad, who have taught, encouraged, and loved me unconditionally. Without your care, I would have significantly more than 7 white hairs.

Acknowledgements to the PSE&G Institute for Sustainability Studies for partially funding this project.

Table of Contents

| | |
|---|-------------|
| <i>Abstract</i> | <i>i</i> |
| <i>Acknowledgments</i> | <i>v</i> |
| <i>List of Figures</i> | <i>vii</i> |
| <i>List of Tables</i> | <i>viii</i> |
| Introduction | 1 |
| 1.1 Literature Review | 3 |
| 1.1.1 Model Appraisal..... | 3 |
| 1.1.2 Bias Correction..... | 5 |
| 1.1.3 Climatology Indices | 7 |
| 1.2 Study Area | 9 |
| 2. Data and Methods | 11 |
| 2.1 Models | 11 |
| 2.1.1 The PRISM Model | 11 |
| 2.1.2 The MACA model..... | 13 |
| 2.1.3 R Statistical Software | 15 |
| 2.2 Correction Factor | 17 |
| 3. Results and Discussion | 18 |
| 3.1 Historical Data Analysis | 18 |
| 3.2 Bias Correcting Historical Data | 23 |
| 3.2.1 Precipitation | 23 |
| 3.2.2 Temperature..... | 29 |
| 3.2.3 Future 4.5 and 8.5 RCP | 30 |
| 3.3 Climatology | 30 |
| 3.3.1 Historic Temperature | 30 |
| 3.3.2 Precipitation and Droughts | 32 |
| 3.4 Future Changes in Extreme Climate Indices to the PRB | 43 |
| 3.4.1 Temperature..... | 43 |
| 3.4.2 Precipitation..... | 45 |
| 4. Discussion | 54 |
| 5. Potential Sources of Error | 57 |
| 6. Conclusion | 57 |
| References | 59 |

List of Figures

| | |
|---|----|
| FIGURE 1-THE PASSAIC RIVER BASIN, LOCATED BETWEEN NEW JERSEY AND NEW YORK STATE..... | 10 |
| FIGURE 2 - LOCATIONS OF CHOSEN STATIONS IN THE PRB STUDY SITE WATERSHED..... | 11 |
| FIGURE 3 – STEPS TAKEN TO MAKE A CLIMATE IMPACT ASSESSMENT FOR THE PRB..... | 11 |
| FIGURE 4 – BIAS CORRECTION OF GCM DATA IN MACA (ABATZOUGLOU, 2013)..... | 14 |
| FIGURE 5 – CDFs OF EACH MACA MODEL AGAINST PRISM..... | 25 |
| FIGURE 6 – CDFs OF THE RAW DATA AND CORRECTED DATA AGAINST PRISM..... | 27 |
| FIGURE 7 – COMPARISON OF SEASONAL AVERAGE PRECIPITATION FOR WINTER AND SUMMER MONTHS WITH CORRELATIONS..... | 28 |
| FIGURE 8 – TMIN, TMAX MONTHLY COMPARISON WITH CORRELATION COEFFICIENT..... | 30 |
| FIGURE 9 – TN10P ANOMALIES..... | 31 |
| FIGURE 10 – TN90P ANOMALIES..... | 32 |
| FIGURE 11 - RAW CDD ANOMALIES..... | 33 |
| FIGURE 12 - CORRECTED CDD ANOMALIES..... | 33 |
| FIGURE 13 - CDD TRENDS USING RAW DATA..... | 34 |
| FIGURE 14- CDD TRENDS USING CORRECTED DATA..... | 35 |
| FIGURE 15 – R10 ANOMALIES USING RAW DATA..... | 36 |
| FIGURE 16 - R10 ANOMALIES USING CORRECTED DATA..... | 36 |
| FIGURE 17 - R10 TRENDS USING RAW DATA..... | 37 |
| FIGURE 18 - R10 TRENDS USING CORRECTED DATA..... | 37 |
| FIGURE 19 – R95P ANOMALIES USING RAW DATA..... | 38 |
| FIGURE 20 - R95 ANOMALIES USING CORRECTED DATA..... | 39 |
| FIGURE 21- R95P TRENDS USING RAW DATA..... | 40 |
| FIGURE 22- R95P TRENDS USING CORRECTED DATA..... | 40 |
| FIGURE 23- Rx5DAY ANOMALIES USING RAW DATA..... | 41 |
| FIGURE 24 - Rx5DAY ANOMALIES USING CORRECTED DATA..... | 42 |
| FIGURE 25 - Rx5DAY TRENDS USING RAW DATA..... | 42 |
| FIGURE 26 - Rx5DAY TRENDS USING CORRECTED DATA..... | 43 |
| FIGURE 27 – CHANGES IN TN10P..... | 44 |
| FIGURE 28 – CHANGE IN TN90P..... | 45 |
| FIGURE 29 – RAW CDD FOR THE THREE MODELS IN EMISSIONS SCENARIOS 4.5 AND 8.5..... | 46 |
| FIGURE 30 - CORRECTED CDD FOR THE THREE MODELS IN EMISSIONS SCENARIOS 4.5 AND 8.5..... | 46 |
| FIGURE 31 – CHANGES IN CDD..... | 47 |
| FIGURE 32 - RAW R10 FOR THE THREE MODELS IN EMISSIONS SCENARIOS 4.5 AND 8.5..... | 48 |
| FIGURE 33 – CORRECTED R10 FOR THE THREE MODELS IN EMISSIONS SCENARIOS 4.5 AND 8.5..... | 48 |
| FIGURE 34 – CHANGE BETWEEN FUTURE AVERAGE R10 RELATIVE TO AVERAGE HISTORICAL R10..... | 49 |
| FIGURE 35 – CHANGES IN R95P..... | 52 |
| FIGURE 36 – CHANGES IN Rx5DAY..... | 53 |
| FIGURE 37 – AVERAGE HISTORICAL (1981-2005) SUMMER AND WINTER PRECIPITATION (MM) FROM OBSERVED (PRISM) AND MACA MODELS. THE ORANGE AREAS REPRESENT PRECIPITATION AMOUNTS RANGING FROM 2-3 MM; YELLOW AREAS REPRESENT PRECIPITATION AMOUNTS RANGING FROM 3-4 MM; THE GREEN AREAS REPRESENT PRECIPITATION AMOUNTS RANGING FROM 4-5 MM..... | 50 |
| FIGURE 38 - PROJECTED CHANGES IN HEAVY WET-WEATHER DAYS IN WHICH PRECIPITATION IS GREATER THAN 10 MM (R10) IN RCP 8.5..... | 51 |
| FIGURE 39 – PROJECTED TRENDS OF MAXIMUM CONSECUTIVE 5-DAY PRECIPITATION IN EMISSIONS SCENARIO RCP 8.5..... | 54 |

List of Tables

| | |
|---|----|
| TABLE 1 – GCM MODELS USED IN THIS STUDY | 15 |
| TABLE 2 – LIST OF POSSIBLE CLIMATE INDICES AVAILABLE FROM THE RCLIMDEX PROGRAM TO BE CALCULATED IN R..... | 17 |
| TABLE 3 - R, R ² , AND ROOT MEAN SQUARE ERROR VALUES FOR THE PRISM MODEL VALUES AND THE OBSERVED DATA. | 19 |
| TABLE 4 – CALCULATED STATISTICS (R, R ² , AND ROOT MEAN SQUARE ERROR VALUES) FOR THE DIFFERENT LOCATIONS CHOSEN. HIGHLIGHTED VALUES SHOW THE BEST R ² VALUES (CLOSEST TO 1)..... | 20 |
| TABLE 5– STATISTICS OF MONTHLY PRECIPITATION BETWEEN 8 MACA MODELS AND PRISM FOR PRECIPITATION AT BLOOMINGDALE, 1981-2005. HIGHLIGHTED VALUE REPRESENTS VALUE CLOSEST TO 1. | 21 |
| TABLE 6 – CORRELATION OF MACA MODEL CNRM-CM5 WITH PRISM IN BLOOMINGDALE | 21 |
| TABLE 7 – STATISTICS FOR THE HAYDEN ISLAND RAIN GAUGE..... | 22 |
| TABLE 8 – STATISTICS FOR THE INTERPOLATED PRISM VALUES AGAINST BCC-CSM1-1M, MRI-CGCM3, AND CCSM4 | 23 |
| TABLE 9 – DAILY CORRECTED CORRELATIONS | 24 |
| TABLE 10 – CORRELATION BETWEEN RAW MACA AND CORRECTED MACA PRECIPITATION..... | 24 |
| TABLE 11 – CORRELATIONS BETWEEN RAW BCC-CSM1-1M, CF CORRECTED BCC-CSM1-1M, AND QMAP-CORRECTED BCC-CSM1-1M DATA TO PRISM | 25 |
| TABLE 12 - STATISTICS OF CORRECTED AND UNCORRECTED TMIN AND TMAX..... | 29 |

Introduction

Climatic patterns are expected to drastically change across the globe during this century. 1983-2012 was the hottest 30-year period in the northern hemisphere in the last 1400 years with this trend continuing to present day (IPCC , 2013). The Northeastern United States is expected to experience significant impacts from climate change with predictions of longer summers, warmer winters, more temperature extremes in the winter and summer, as well as increased occurrence of droughts despite expectations of more frequent, heavier wet-weather events (Karl, et al., 2009). The magnitude of these predicted changes can vary greatly, even for neighboring townships. Therefore, although scientists can predict the effects of climate change on large areas using Global Climate Models (GCMs), impacts may differ on the local level (NASA, 2018), in which case Regional Climate Models (RCMs) may be beneficial.

Global Climate Models (GCMs) are very useful tools for predicting climate. They can predict the changes in climate variables including minimum temperature, maximum temperature, precipitation, relative and specific humidity, wind speed, and solar radiation. They can also determine the changes in these variables based on several greenhouse gas concentration scenarios. These scenarios, known as the Representation Concentration Pathways (RCP), predict the impact of climate change under four main scenarios: RCPs 2.6, 4.5, 6, and 8.5. RCP2.6 represents the “best case” and most unlikely path in which greenhouse gases (GHGs) emissions are heavily regulated and decline after 2020, while RCP8.5 represents a scenario on the other side of the spectrum, in which emissions continue unregulated and rise until 2100. RCPs 4.5 and 6 represent more moderate scenarios, or “stabilization pathways,” with radiative forcing of 4.5 W/m² and 6 W/m² respectively. In these situations, emissions reach a peak during the middle of the century before balancing out (IPCC Climate Report, 2007).

GCMs provide information on several climatic variables, but they do not often provide accurate data at horizontal scales smaller than 5 kilometers (Kim, et al., 2016). In order to make these large-scale and coarse datasets more accurate, Regional Climate Models (RCMs) such as the Multivariate Adaptive Constructed Analogs (MACA) model perform downscaling and bias-correction under different emissions scenarios for historical and future projections. Downscaling refers to the process of using large-resolution data to fit a finer scale resolution. However, with downscaling comes some amount of uncertainty. To deal with the pre-existing bias and consequent uncertainty from downscaling, researchers also employ bias correction. Bias correction involves adjusting data output through statistical analysis. By downscaling and bias-correcting climate data from GCMs, more accurate projections concerning specific localities can be made.

The Passaic River Basin (PRB) provides an interesting study site. Because of the concentrated population, the pervious area in the PRB, particularly in the areas closer to New York City, has decreased (Rutgers University Center for Remote Sensing and Spatial Analysis, 2009). A largely impervious surface area indicates increased tendency for flooding as stormwater enters waterbodies more quickly with more intensive destructive force. Decreased permeability also suggests an increased impact of the “heat island” effect. The heat island effect refers to the phenomenon that occurs after vegetated areas are replaced by grey infrastructure. The previously vegetated areas experience the impact of lower albedo; instead of reflecting solar radiation, dark concrete can absorb anywhere from 60 to 95% of the solar energy reaching it, therefore generating more heat for the surrounding area (Environmental Protection Agency, 2012). In urban regions, this effect can increase grey surface temperature by 50-90°F (27-50°C) during the day and up to 22°F (12°C) at night (Environmental Protection Agency, 2017). Therefore, further bias correction

of raw data is necessary to include the impact of grey infrastructure on local temperatures (among other sources of inaccuracy).

This thesis investigates the usefulness of applying MACA data to predict the impacts of climate change in the whole of the PRB under emission scenarios RCP 4.5 and RCP 8.5 after performing further bias correction. The study looks at several ways in which the PRB will experience precipitation and temperature changes. Identifying future changes in the PRB with respect to the coldest nights, warmest nights, consecutive dry days, rainy days in which precipitation exceeds 10 mm, the 95th percentile of precipitation, and the yearly maximum consecutive 5-day precipitation can be useful to planners and policy makers to help communities increase their resilience against climate change.

1.1 Literature Review

1.1.1 Model Appraisal

Multivariate Adaptive Constructed Analogs (MACA)

Before collecting raw data from MACA, model validation was key; why would MACA be a better model to provide data over the other available Regional Climate Models (RCMs)? Several other RCMs also offer statistically downscaled climate data. For example, the Bias-Correction Spatial Disaggregation (BCSD), Bias-Correction/Constructed Analogue (BCCA), and Bias-Correction/Climate Imprint (BCCI) all provide daily precipitation, minimum and maximum temperature simulations through statistical downscaling. In one comparison of the aforementioned models over the entirety of South Korea, MACA delivers the best overall statistical results for historical temperature and precipitation (Eum, et al., 2017). Though other studies find MACA to be less accurate in their respective study areas, the error found did not prove to be enough of a deterrent to look towards other models (Demirel & Moradkhani, 2016).

Ultimately, MACA proves to be a preferable RCM to provide daily historical and future climate output for several reasons. It preserves climatic trends from GCM data using a 31-year smoothing window, bias-corrects precipitation and temperature data, and uses a reduced set of analog patterns while including information from older analogs (Mote, et al., 2015). Perhaps the greatest strength of the MACA model lies in its ability to spatially downscale data from observed data rather than to use interpolation. Additionally, MACA is able to relate separate variables together to produce better results; by downscaling temperature with precipitation, MACA obtains better results for historical snowfall amounts. These factors all qualify MACA as a preferred climate downscaling model.

Parameter-elevation Regressions on Independent Slopes Model (PRISM)

Ten locations in the PRB were chosen to represent the overall impact of climate change in the study area. These locations were chosen based on available rain gauges; however, despite choosing locations with rain gauges assigned by the USGS, only 3 out of 10 locations had usable historical precipitation data that overlapped with the chosen time frame of January 1981 to December 2005. Furthermore, there was almost no temperature data for these locations. Therefore, it was necessary to find an accurate model that could produce observed precipitation and temperature values to compare to the historical MACA data.

The Parameter-elevation Regressions on Independent Slopes Model (PRISM) model developed at Oregon State University provides historical data for several variables at chosen spatial and temporal resolutions. PRISM provides daily temperature and precipitation data at 800-m and 4-km resolutions and therefore matches well to the 4-km resolution MACA data. Studies comparing PRISM to other gridded network models also found PRISM to be highly reliable, with other models overestimating precipitation in areas with vastly varied topographies (Kim, et al.,

2017). The mean average error (MAE, %) and the bias (%), as calculated below, provided a statistical basis on which the datasets could be compared:

$$MAE = \frac{1}{n} \sum_{i=1}^n |y_i - x_i| \quad (1)$$

where n represents the count of data points, y is the observed data point, and x is the model value, and:

$$Bias = \frac{Observed - Model}{Model} \times 100 \quad (2)$$

Compared with two different observation datasets, another study found a maximum of 5.25% MAE and a maximum bias of 1.5%, therefore validating the PRISM dataset for the study (Daly, et al., 2017).

1.1.2 Bias Correction

Generated data from climate models benefit from further bias-correction, regardless of the bias-correction embedded in the model code. Because of the bias that may come from inaccuracies in the original GCMs—equations that cannot possibly universally accurately cover the Earth’s surface, models that cannot fully capture everyday physics—model data must be corrected for higher statistical correlation. Quantile mapping is perhaps the most commonly used method of bias correction.

A cumulative distribution function (CDF) can better relate model data to observed data. The CDF, or the cumulative distribution of a dataset, can be extremely helpful in data analysis. The x-value of a cumulative distribution function graph shows the quantity of the data being measured—in this study, millimeters of precipitation—while the y-value on the CDF plot represents the percentage of data that has a value smaller than or equal to the corresponding x value (Data Camp, 2016). Because the y-value is the accumulation of data points at the corresponding x-value, the y-value will never reach more than 1 (or 100%). CDFs represent the

area underneath the probability distribution curve; therefore, if $f(t)$ represents the probability density function, the CDF $F(t)$ can be represented as:

$$F(t) = \int_{-\infty}^x f(t)dt \quad (3)$$

Using this equation, we can then bias-correct using a transfer function:

$$\hat{x}_m(t) = F_O^{-1}[F_m\{x_M(t)\}] \quad (4)$$

where $\hat{x}_m(t)$ is the bias-corrected data, $x_m(t)$ represents the model data, F_O^{-1} is the inverse of the observed CDF and F_m is the model CDF (Eum, et al., 2017). This formula helps shift the modeled values to more closely match the observed values based on the cumulative probability of occurrence. This method, called quantile mapping, is extremely sophisticated and suggests that when the model CDFs more closely match the observed—in that they have similar distribution curves—the values and resulting analysis have higher credibility. Comparing the CDFs of observed and model data can be helpful in proving the reliability of employed correction methods.

Another useful method of historical data correction is the linear scaling correction factor method, which differs between precipitation and temperature. For precipitation, corrections were made by a multiplicative factor consisting of the ratio between observed and model values applied to daily observed values:

$$c = \frac{\sum_{i=1}^n P_i^{obs}}{\sum_{i=1}^n P_i^{model}} \quad (5)$$

$$\widetilde{P}_{ij}^{model} = c * P_{ij}^{model} \quad (6)$$

where c is the correction factor, P_i^{obs} is the mean monthly observed precipitation, P_i^{model} is the monthly mean of the model value of precipitation, and $\widetilde{P}_{ij}^{model}$ is a daily timeseries value for the corrected model data (Hempel, et al., 2013). This method, although simple, is useful in correcting

precipitation data. In using the correction factor, a monthly mean over the baseline period is calculated and applied to daily values (Chen, et al., 2013).

The temperature, however, is corrected in a slightly different way. While precipitation is corrected by more complex functions due to higher GCM error in capturing precipitation, temperature bias correction is calculated through additive correction because of the simpler patterns in temperature fluctuations:

$$C = \frac{1}{n} (\sum_{i=1}^n T_i^{obs} - \sum_{i=1}^n T_i^{model}) \quad (7)$$

$$\widetilde{T}_{ij}^{model} = C + T_{ij}^{model} \quad (8)$$

where C is the correction factor, n is the total number of days in the defined time period, T_i^{obs} is the observed temperature at day i , T_i^{model} is the modeled output temperature at day i , and $\widetilde{T}_{ij}^{model}$ is the corrected temperature at day i in month j (Hempel, et al., 2013).

Finally, the future values must also be corrected for potential bias. In this study, we will apply the correction factors to daily model output for the time period 2051-2075.

1.1.3 Climatology Indices

Climatology indices can be extremely helpful in identifying the ways climate is expected to change with regards to global warming. Several studies analyze changes in their respective study areas by identifying several key climate indices. Marengo et al. look at very cold nights, very warm nights, consecutive dry days, maximum 5-day precipitation, extreme rainfall, and wet days as part of their analysis of changes in climate extremes for South Africa (Marengo, et al., 2009). In their study, Marengo et al. use other RCMs to compare climate extremes from a baseline period of 1961-1990 against the projected extreme from 2071-2100. Thibeault & Seth employ comparable methods of comparison of similar climate extremes between a baseline period of 1981-2010 and

projected future trends from 2041-2070, informing our methods of climatology analysis (Thibeault & Seth, 2004).

The Northeastern part of the United States is already prone to cold streaks, heatwaves, heavy precipitation, flooding events, and droughts (Thibeault & Seth, 2014). Heatwaves, combined with heavy humidity characteristics of the PRB, can lead to dangerous situations for human health and wellbeing as well as for implemented infrastructure. Cold streaks can do equal amounts of damage; by investigating the predicted change in extreme temperature lows compared with historical lows, warming trends can be verified. Therefore, predictions of future changes in extreme temperature and precipitation events will serve as a backbone of decision support for creation of policy to increase community resilience.

The goal of this study is to employ state-of-the-science methods and data to analyze potential future changes in several climate extreme indices for the PRB, including:

- (1) very cold nights (TN10p), where the percentage of time in a year when daily minimum temperature falls below the 10th percentile of the daily temperature of the reference period and future period;
- (2) very warm nights (TN90p) that are above the 90th percentile of minimum temperature;
- (3) consecutive dry days (CDD), in which the annual maximum number of consecutive days when daily precipitation falls less than 1 mm;
- (4) maximum 5-day precipitation (R5xday), the maximum consecutive total precipitation within a 5-day window within a defined amount of time;
- (5) amount of days in which precipitation is over 10 mm (R10); and
- (6) extreme precipitation (R95P), the annual total precipitation in which precipitation is above the 95th percentile of the defined time period's daily distribution.

It is important to note that these climate indices are not determined by a universal standard because of the variations in climate across the globe. The results in Section 3 pertain only to the PRB and cannot necessarily be extended to the larger New Jersey or northeastern US region without further analysis.

1.2 Study Area

The PRB encompasses and drains approximately 935 square miles of land largely in New Jersey and partially in southern New York State (see Figure 1). The area was heavily influenced by the Wisconsin Ice sheet, which melted about 11,000 years ago (Passaic River Basin, 2016). Nestled in the basin is the Passaic River, which empties out into the Newark Bay at 80 miles (129 kilometers) from the source. The river has played an important role in development within the basin in the last few centuries. Thousands of people settled along the Passaic River in the late 1700s with the successful silk industry inviting laborers and business-minded people alike to the area. Additionally, because a majority of the PRB is also considered to be part of metropolitan New York City, the PRB has become an attractive location for commuters. The steady increase in population since the 1700s has led to the PRB being one of the most densely populated regions in the most densely populated state.

The area in which the rain gauges are located comprises a subwatershed in the PRB. The elevation in this area ranges from 91 feet to 1462 feet—a slight difference from the larger PRB, which ranges from 21 to 1480 feet. The highest values correspond to the Highlands. The PRB is particularly vulnerable to climate extremes such as floods and heat waves. Expected global warming-induced changes in climate extremes into the future are therefore of particular concern for PRB. Detailed analysis of potential future changes in climate extremes for PRB using state-of-the-art climate model projections is still lacking; therefore, this study hypothesizes that the

application of new high-resolution climate data will provide better information on plausible future changes in extremes.

This area is also of particular importance because of the water that the Highlands provides to New Jersey residents. The Highlands provide nearly 66% of New Jersey residents with clean drinking water. Therefore, looking at the impact of climate change on this area is of great importance for future generations.

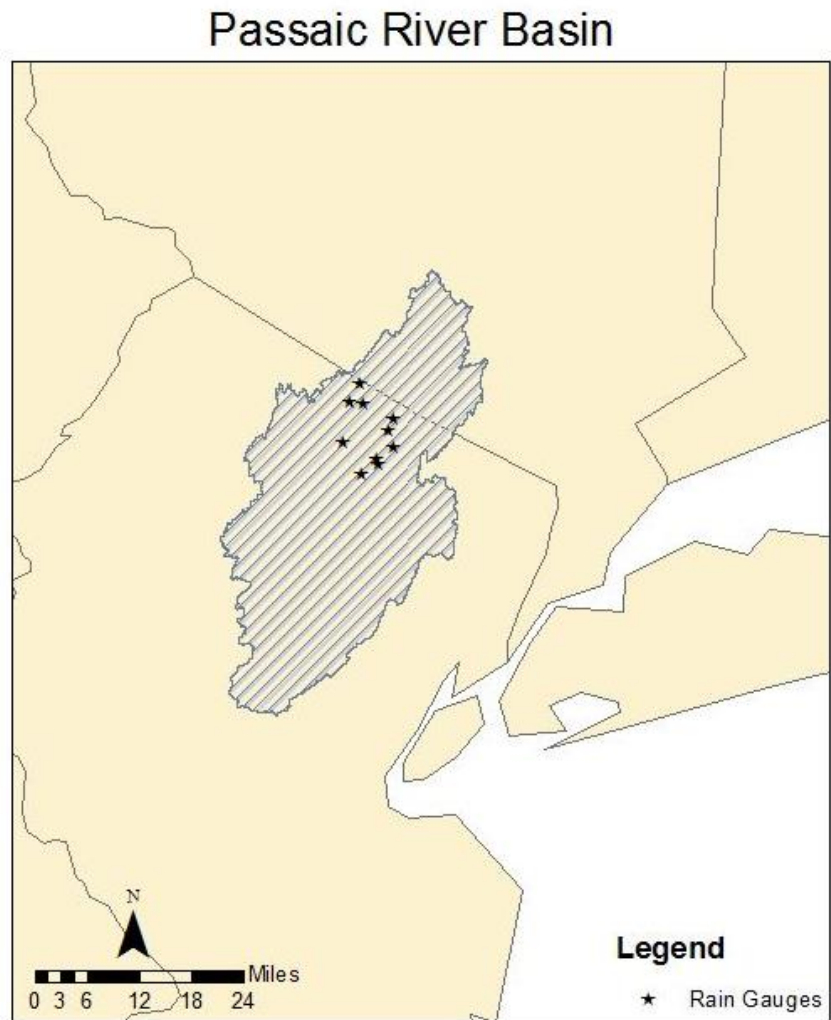


Figure 1-The Passaic River Basin, located between New Jersey and New York State

For this study, ten (10) locations were determined as reasonable points of interest (see

Figure 2 below) due to the available rain gauges and precipitation data at the chosen locations. The available historical precipitation data came from the USGS.

| FID | Stations | Lon | Lat | Start | End |
|-----|---------------------------------|-----------|----------|---------------|--------------|
| 12 | BLOOMINGDALE 0.7 SSE, NJ US | -74.3289 | 41.0202 | 11/30/14 0:00 | 6/4/17 0:00 |
| 14 | GREENWOOD LAKE, NJ US | -74.32444 | 41.13861 | 1/1/41 0:00 | 3/31/09 0:00 |
| 16 | RINGWOOD 1.0 ENE, NJ US | -74.2575 | 41.1107 | 5/30/09 0:00 | 7/9/11 0:00 |
| 17 | RINGWOOD 3.0 SSE, NJ US | -74.2571 | 41.0653 | 7/10/11 0:00 | 6/2/17 0:00 |
| 18 | RINGWOOD, NJ US | -74.2683 | 41.0917 | 1/1/02 0:00 | 9/30/13 0:00 |
| 19 | WANAQUE 0.6 S, NJ US | -74.2892 | 41.0351 | 7/1/10 0:00 | 7/16/14 0:00 |
| 20 | WANAQUE RAYMOND DAM, NJ US | -74.2933 | 41.0444 | 8/1/45 0:00 | 6/1/17 0:00 |
| 21 | WEST MILFORD TWP 2.5 SSE, NJ US | -74.368 | 41.0739 | 9/4/10 0:00 | 6/3/17 0:00 |
| 22 | WEST MILFORD TWP 3.2 NE, NJ US | -74.3536 | 41.141 | 4/27/10 0:00 | 6/16/13 0:00 |
| 23 | WEST MILFORD TWP 5.5 NE, NJ US | -74.3293 | 41.1705 | 1/3/10 0:00 | 1/28/13 0:00 |

Figure 2 - Locations of chosen stations in the PRB study site watershed

2. Data and Methods

Several models were used in collecting and processing data for this study. The following section details the steps used in this study (see Figure 3 – Steps taken to make a climate impact assessment for the PRB).

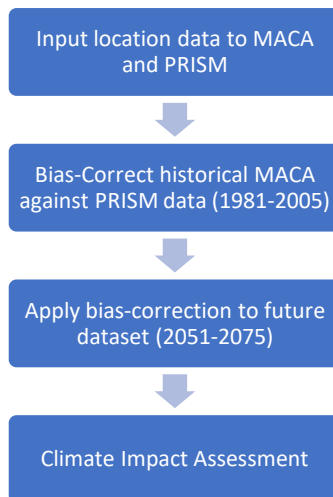


Figure 3 – Steps taken to make a climate impact assessment for the PRB

2.1 Models

2.1.1 The PRISM Model

The PRISM model was created by a team of researchers under the Northwest Alliance for Computational Science and Engineering (NACSE) at Oregon State University. PRISM provides daily and monthly estimates of precipitation (measured as the total daily or monthly amount of rainfall and melted snow), minimum temperature, maximum temperature, mean dew point, minimum mean dew point, minimum vapor pressure deficit, and maximum vapor pressure deficit (PRISM, 2016). These datasets are freely available at <http://www.prism.oregonstate.edu/>.

PRISM offers data for the aforementioned variables ranging from 1895 to present day. For the “historical” data, monthly values are offered from 1895 to 1980, whereas daily and monthly data for more recent years are available from 1981 to present day. These recent time series data are formulated using climatologically-aided interpolation (CAI). CAI uses 30-year averages to determine the spatial pattern of a chosen point location or specified area by using an algorithm to create a relationship between elevation, climate, and station data for individual grid cells. It has also recently incorporated proximity to coastlines, complexity of local terrain, and potential for temperature inversions to its algorithm (Daly & Bryant, 2013). PRISM performs climate-elevation regressions using a complex network of stations and a layered algorithm to produce climate data for the conterminous United States.

PRISM data is available in several formats, but for the purposes of the study, data was obtained in the form of a comma-separated value (.csv) worksheet to be read in Excel (for point locations) and band interleaved line (.bil), to be extracted in GIS or other available software. Daily values for precipitation and temperatures from January 1, 1981 until December 31st, 2005 were chosen in order to match the time series available from MACA (see Section 2.1.2 – The MACA Model). Downloaded data provided metric units to also match the time series from MACA in order to ensure the maximum preservation of raw data.

2.1.2 The MACA model

The MACA model (Abatzoglou, 2013) was developed at the University of Idaho. This model uses statistical downscaling instead of dynamic downscaling. Dynamic downscaling requires the use of high-resolution climate models at the regional level to produce data, with an observational or lower-resolution climate data as a “boundary condition” (National Center for Atmospheric Research, 2018). MACA developers, on the other hand, used statistical downscaling to create an algorithm relating local climate variables (precipitation, temperature, humidity, etc.) to each other and then to existing global climate model data.

The MACA process is lengthy, requiring several steps to produce the final output. First, a “training” or observational dataset for each variable is determined. For the METDATA used in this study, a training period of daily data from the NASA North American Land Data Assimilation System (NLDAS-2) for the time period of 1979-2012 was used. The datasets are then interpolated to a 1° x 1° grid from larger resolution grids, after which point they undergo “epoch adjustment” and are adjusted to predict seasonal and yearly trends. Bias-correction of the training dataset is performed using monthly PRISM values for temperature, precipitation, and humidity. Output is validated against several other weather station data sources (MACA, 2013).

MACA then takes data from the GCMs to compare to the training dataset. These GCMs are coordinated by the Coupled Model Inter-Comparison Model 5 (CMIP5) and provide metadata to climatologists worldwide and is a significant, trusted source of data; the United Nations released a report on the expected impacts of climate change by heavily relying on the information provided by the CMIP5 GCM datasets. MACA utilizes 20 of the GCMs to run because of various incompatibilities with the excluded models.

A cumulative distribution function plot for the GCM and training data is created for each grid and through use of equidistant quantile mapping of the future GCM data, adjustments are made with quantile differences in the CDFs preserved. These adjustments are the bias-correction of the data (see Figure 4 – Bias Correction of GCM data in MACA (Abatzoglou, 2013)).

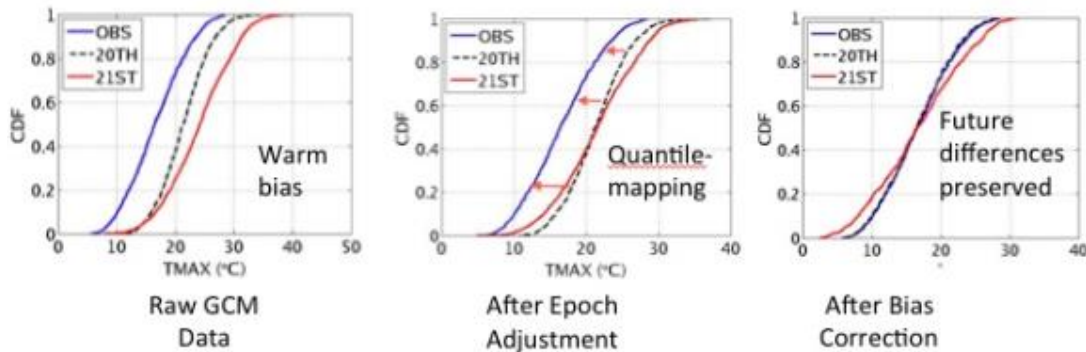


Figure 4 – Bias Correction of GCM data in MACA (Abatzoglou, 2013)

After the data is corrected, the statistical distribution of the GCM matches the statistical distribution from the training dataset and the spatial resolution of the output data will also match the resolution of the training set. After some more fine-tuning and minor bias-correction, the data are ready. It is important to note that although the statistical distribution of the model more closely matches the statistical distribution of the training dataset, MACA is not intended to be used as a hindcast of historic weather. Therefore, observational data from 1990 does not exactly correlate to the MACA data from 1990.

For purposes of this study, three GCMs were chosen to provide historical and future climate data: (1) bcc-csm1-1m, (2) MRI-CGCM3, and (3) CCSM4 (see Table 1 – GCM Models used in this study). These models represent 3 of 30 ranked GCMs, all of which have significantly differing normalized error score. The normalized error comes from 18 performance analytics for a study area in the Pacific Northwest. The most accurate, in which the normalized error score is closest to 0, is CCSM4, which is ranked as the 3rd most accurate model in terms of normalized error. Bcc-

csm1-1m falls next at 13 and MRI-CGCM3 ranks 27 (Rupp, et al., 2013). With such a wide range of performance, this study can obtain a fuller understanding of possible future climatic changes.

| Model | Center | Country | Resolution |
|--------------------|---|----------------|-------------------|
| bcc-csm1-1m | Beijing Climate Center | China | 1.12° x 1.12° |
| CCSM4 | National Center of Atmospheric Research | USA | 1.25° x 0.94° |
| MRI-CGCM3 | Meteorological Research Institute | Japan | 1.1° x 1.1° |

Table 1 – GCM Models used in this study

2.1.3 R Statistical Software

This study uses R Statistical Software, a program maintained by the R Foundation for Statistical Computing. Two software packages were installed for use in this study.

Qmap version 1.0-4, a package created by Lukas Gudmundssen at the Institute of Atmosphere and Climate Science in Zürich, was used to determine quantile mapping for bias-correction of downloaded data. Qmap offers several methods of bias-correction. Because the function “qmapDIST” most closely fit the quantile mapping correction methods used in the literature (see Section 1.1.2 Bias Correction), qmapDIST was chosen as the best approach towards bias correction of the model data. QmapDist creates a function in which the inverse CDF of the observed dataset—or the corresponding quantile function from the observed dataset—becomes a function of the model CDF at a daily data point, x :

$$\hat{x}_m(t) = F_O^{-1}[F_m\{x_M(t)\}]$$

Qmap consists of two primary steps: fitqmapDIST and doQmapDIST. FitqmapDIST is the command used to relate observed and modelled time series data, while doQmapDIST transforms the model data using the transformation algorithm from fitQmapDIST (Gudmundssen, 2016).

These functions were key in producing daily time series for the quantile mapping method of data correction.

The second R package referenced in this study is the RCLimDex package. RCLimDex is a package created by a team of researchers at the Climate Change Research Centre (CCRC) at the University of New South Wales (UNSW). RCLimDex is programmed to identify 27 climate indices (see Table 2 – List of possible climate indices available from the RCLimDex program to be calculated in R) (ClimDEX, 2013).

| Notation | Name | Definition |
|-----------------------|--|--|
| FD | Frost Days | Annual count of days where the minimum temperature (TN) is less than 0°C TN_{ij} is daily min temp on day i, year j $TN_{ij} < 0^{\circ}C$ |
| SU | Summer Days | Annual count of days where maximum (TX) temperature is greater than 25°C TX_{ij} is the daily max temp on day i, year j $TX_{ij} > 25^{\circ}C$ |
| ID | Icing Days | Annual count of days where maximum temperature is less than 0°C $TX_{ij} < 0^{\circ}C$ |
| TR | Tropical Nights | Annual count of days where minimum temperature is greater than 20°C $TN_{ij} > 20^{\circ}C$ |
| GSL | Growing Season Length | Annual count of first span of at least 6 days with daily mean temperature (TG) greater than 5°C and span of 6 days after July 1 st where TG is less than 5°C $TG_{ij} > 5^{\circ}C$ <i>After July 1: $TG_{ij} < 5^{\circ}C$</i> |
| TX_x | Monthly Max Value of Daily Max Temp | Daily maximum temperatures in month k, period j $TX_{xkj} = \max(TX_{xkj})$ |
| TN_x | Monthly max value of daily min temp | Daily minimum temperatures in month k, period j $TN_{xkj} = \max(TN_{xkj})$ |
| TX_n | Monthly min value of daily max temp | Daily maximum temperatures in month k, period j $TX_{nkj} = \min(TX_{nkj})$ |
| TN_n | Monthly min value of daily min temp | Daily minimum temperatures in month k, period j $TN_{nkj} = \min(TN_{nkj})$ |
| TN10p | Percentage of days when TN < 10 th percentile | TN_{in10} is the calendar day where the 10 th percentile is centered on a 5-day window for the base period 1961-1990 $TN_{ij} < TN_{in10}$ |
| TX10p | Percentage of days when TX < 10 th percentile | TX_{in10} be the calendar day 10 th percentile centered on a 5-day window for the base period 1961-1990 $TX_{ij} < TX_{in10}$ |
| TN90p | Percentage of days when TN > 90 th percentile | TN_{in90} be the calendar day 90 th percentile centred on a 5-day window for the base period 1961-1990 $TN_{ij} > TN_{in90}$ |
| TX90p | Percentage of days when TX > 90 th percentile | TX_{in90} be the calendar day 90 th percentile centred on a 5-day window for the base period 1961-1990 $TX_{ij} > TX_{in90}$ |
| WSDI | Warm spell duration index | Annual count of days with at least 6 consecutive days when TX > 90 th percentile $TX_{ij} > TX_{in90}$ |
| CSDI | Cold spell duration index | Annual count of days with at least 6 consecutive days when TN < 10 th percentile $TN_{ij} < TN_{in10}$ |
| DTR | Daily temp range | Monthly mean difference between TX and TN |
| Rx1day | Monthly maximum 1-day precipitation | Let RR_{ij} be the daily precipitation amount on day i in period j. The maximum 1-day value for period j are: $Rx1day_j = \max(RR_{ij})$ |
| Rx5day | Monthly max consecutive 5-day precip | Let RR_{kj} be the precipitation amount for the 5-day interval ending k, period j. Then maximum 5-day values for period j are: $Rx5day_j = \max(RR_{kj})$ |

| | | |
|----------------|---|---|
| SDII | Simple precip intensity index | The daily precipitation amount on wet days, w ($RR \geq 1\text{mm}$) in period j . If W represents number of wet days in j , then: $SDII = (\sum RR_{w,j})/W$ |
| R10mm | Annual count of days when $PRCP \geq 10\text{mm}$ | Let RR_{ij} be the daily precipitation amount on day i in period j . Count the number of days where: $RR_{ij} \geq 10\text{mm}$ |
| R20mm | Annual count of days when $PRCP \geq 20\text{mm}$ | Let RR_{ij} be the daily precipitation amount on day i in period j . Count the number of days where: $RR_{ij} \geq 20\text{mm}$ |
| Rnmm | Annual count of days when $PRCP \geq n\text{mm}$ | n is a user defined threshold: Let RR_{ij} be the daily precipitation amount on day i in period j . Count the number of days where: $RR_{ij} \geq n\text{mm}$ |
| CDD | Maximum length of dry spell | Let RR_{ij} be the daily precipitation amount on day i in period j . Count the largest number of consecutive days where: $RR_{ij} < 1\text{mm}$ |
| CWD | Maximum length of wet spell | Let RR_{ij} be the daily precipitation amount on day i in period j . Count the largest number of consecutive days where: $RR_{ij} \geq 1\text{mm}$ |
| R95pTOT | Annual total PRCP when $RR > 95p$ | Let $RR_{w,j}$ be the daily precipitation amount on a wet day w ($RR \geq 1.0\text{mm}$) in period i and let $RR_{wn,95}$ be the 95 th percentile of precipitation on wet days in the 1961-1990 period. If W represents the number of wet days in the period, then $R95p_i = \sum RR_{w,j}$, where $RR_{w,j} > RR_{wn,95}$, |
| R99pTOT | Annual total PRCP when $RR > 99p$ | Let $RR_{w,j}$ be the daily precipitation amount on a wet day w ($RR \geq 1.0\text{mm}$) in period i and let $RR_{wn,99}$ be the 99 th percentile of precipitation on wet days in the 1961-1990 period. If W represents the number of wet days in the period, then: $R99p_i = \sum RR_{w,j}$, where $RR_{w,j} > RR_{wn,99}$ |
| PRCPTOT | Annual total precipitation in wet days | Let RR_{ij} be the daily precipitation amount on day i in period j . If i represents the number of days in j , then $PRCPTOT_j = \sum RR_{ij}$ |

Table 2 – List of possible climate indices available from the RClimDex program to be calculated in R

2.2 Correction Factor

One method of historical bias-correction explored in this study is the correction factor method. The correction factor method uses a simple, linear approach toward correction of daily climate data. For this study, daily corrected values are calculated for the baseline period per model by using the equations:

$$c = \frac{\frac{1}{n} \sum_{i=1}^n P_i^{obs}}{\frac{1}{n} \sum_{i=1}^n P_i^{model}}$$

$$\widetilde{P}_{ij}^{model} = c * P_{ij}^{model}$$

where c is the correction factor, P_i^{obs} is the mean monthly observed precipitation, P_i^{model} is the monthly mean of the model value of precipitation, and $\widetilde{P}_{ij}^{model}$ is a daily timeseries value for the corrected model data.

The temperature, however, is corrected in a slightly different way because of the simpler patterns in temperature fluctuations. While precipitation is corrected by a multiplicative factor, the temperature correction factor is calculated through additive methodology:

$$C = \frac{1}{n} \left(\sum_{i=1}^n T_i^{obs} - \sum_{i=1}^n T_i^{model} \right)$$

$$\widetilde{T}_{ij}^{model} = C + T_{ij}^{model}$$

where C is the correction factor, n is the total number of days in the defined time period, T_i^{obs} is the observed temperature at day i , T_i^{model} is the modeled output temperature at day i , and $\widetilde{T}_{ij}^{model}$ is the corrected temperature at day i in month j .

The correlation coefficient R , coefficient of determination R^2 , root mean square error RMSE, and the CDFs were calculated for statistical analysis of the data.

3. Results and Discussion

3.1 Historical Data Analysis

After downloading data from MACA and PRISM, the first step in the analysis was to validate the PRISM data. Historical observed precipitation data from the USGS was only available for 3 locations. Full precipitation comparisons were available for (FID 14) Greenwood Lake and (FID 20) Wanaque Raymond Dam while a partial comparison (Jan 2002 – Dec 2005) was available for (FID 18) Ringwood. Correlations and RMSE were calculated to determine the similarity between for daily PRISM and USGS/NOAA time series data (See Table 3 - R , R^2 , and Root Mean Square Error values for the PRISM model values and the observed data.). Because PRISM had an R^2 range from 0.83-0.99 with the available observed data, and because there was not enough precipitation or temperature data from the USGS—the original designated resource for observed values—PRISM served as a solution to provide observational values.

| Statistics | | | |
|------------------------|---------------|----------------|-----------|
| Location | PRISM vs NOAA | | |
| | r | r ² | RMSE |
| 14 Greenwood Lake | 0.9952145 | 0.99045190 | 0.0121796 |
| 18 Ringwood | 0.9152671 | 0.83771395 | 0.0313515 |
| 20 Wanaque Raymond Dam | 0.9133208 | 0.83415497 | 0.0361998 |

Table 3 - R, R², and Root Mean Square Error values for the PRISM model values and the observed data.

The next step involved inspecting the daily time series values for precipitation, minimum temperature, and maximum temperature for each location (1981-2005) in MACA using bcc-csm1-1m, MRI-CGCM3, and CCSM4. However, looking at the daily values provided little clarity (see

Table 4 – Calculated statistics (R, R², and Root Mean Square Error values) for the different locations chosen. Highlighted values show the best R² values (closest to 1.) towards the correlation between the different models and as such, the data was converted to average monthly values for easier viewing and understanding (see Figure 4 on next page).

There is a high correlation between the models for minimum and maximum values for temperature. Precipitation, however, shows large variations in value, with no single MACA model showing determination correlation (R²) greater than 0.0083 with respect to PRISM values.

For temperature predictions, MRI-CGCM3 consistently shows the highest correlation while CCSM4 shows marginally better R² values in precipitation predictions. In all aspects, bcc-csm1-1m proves to be the least accurate compared to the PRISM model.

Because the correlation between the values produced by the three MACA models and PRISM were so low, data was re-downloaded for each location. The units were double-checked to ensure compatibility, confirmed that MACA and PRISM had the same 4-kilometer resolution, and, as per the MACA website recommendation, which recommended against using only 1 or 2 models (MACA, 2013), increased the number of models number to 9 and the correlation values were still consistently low (see Figure 6).

| Precipitation Statistics | | | | | | | | | |
|-----------------------------|--------------|----------------|-----------|--------------|----------------|-----------|----------------|----------------|-----------|
| Location | BCC vs Prism | | | MRI vs Prism | | | CCSM4 vs Prism | | |
| | r | r ² | RMSE | r | r ² | RMSE | r | r ² | RMSE |
| 12 Bloomingdale | -0.0078953 | 0.0000623 | 0.1052651 | 0.0377433 | 0.0014246 | 0.0957545 | -0.0413468 | 0.0017096 | 0.1051409 |
| 14 Greenwood Lake | 0.0045273 | 0.0000205 | 0.1096398 | 0.0280330 | 0.0007858 | 0.1011030 | -0.0914016 | 0.0083543 | 0.1123264 |
| 16 Ringwood 1.0 ENE | 0.0220498 | 0.0004862 | | 0.0468249 | 0.0021926 | 0.0975641 | -0.0633439 | 0.0040125 | 0.1073260 |
| 17 Ringwood 3.0 SSE | 0.0139878 | 0.0001957 | 0.1052242 | 0.0455966 | 0.0020790 | 0.0968216 | -0.0626746 | 0.0039281 | 0.1073697 |
| 18 Ringwood | 0.0058316 | 0.0000340 | 0.1056735 | 0.0469887 | 0.0022079 | 0.0965897 | -0.0564177 | 0.0031830 | 0.1060237 |
| 19 Wanaque 0.6 S | -0.0121913 | 0.0001486 | 0.1062696 | 0.0401288 | 0.0016103 | 0.0958600 | -0.0359703 | 0.0012939 | 0.1048827 |
| 20 Wanaque Raymond Dam | -0.0056172 | 0.0000316 | 0.1057353 | 0.0379404 | 0.0014395 | 0.0965097 | -0.0371205 | 0.0013779 | 0.1054449 |
| 21 West Milford Twp 2.5 SSE | -0.0106110 | 0.0001126 | 0.1098460 | 0.0144991 | 0.0002102 | 0.1011768 | -0.0704495 | 0.0049631 | 0.1104478 |
| 22 West Milford Twp 3.2 NE | 0.0035132 | 0.0000123 | 0.1106574 | 0.0267016 | 0.0007130 | 0.1015744 | -0.0843010 | 0.0071067 | 0.1124062 |
| 23 West Milford Twp 5.5 NE | -0.0001662 | 0.0000000 | 0.1102944 | 0.0300870 | 0.0009052 | 0.1011672 | -0.0864577 | 0.0074749 | 0.1124217 |

| Tmin Statistics | | | | | | | | | |
|---------------------|-------------|----------------|------------|------------|----------------|------------|------------|----------------|------------|
| location | bcc-csm1-1m | | | CCSM4 | | | MRI-CGCM3 | | |
| | r | R ² | RMSE | r | R ² | RMSE | r | R ² | RMSE |
| Bloomingdale | 0.8047245 | 0.64758152 | 6.00304217 | 0.80321088 | 0.64514772 | 5.99379891 | 0.80699555 | 0.65124182 | 5.88031498 |
| Greenwood Lake | 0.80351295 | 0.64563305 | 6.05813039 | 0.80196522 | 0.64314821 | 6.05475582 | 0.8057863 | 0.64929156 | 5.92578459 |
| Ringwood 1.0 | 0.80666714 | 0.65071188 | 5.9455331 | 0.80510715 | 0.64819752 | 5.94023737 | 0.80903027 | 0.65452998 | 5.82456029 |
| Ringwood 3.0 | 0.80753049 | 0.6521055 | 5.98866252 | 0.80580478 | 0.64932135 | 5.98965064 | 0.80946334 | 0.6552309 | 5.86406571 |
| Ringwood | 0.8074032 | 0.65189993 | 5.99325953 | 0.80582919 | 0.64936068 | 5.99123541 | 0.80948531 | 0.65526647 | 5.86554786 |
| Wanaque 0.6 | 0.8080627 | 0.65296533 | 5.84940721 | 0.80602272 | 0.64967263 | 5.848232 | 0.80949176 | 0.6552769 | 5.76933306 |
| Wanaque Raymond Dam | 0.80838342 | 0.65348376 | 5.84820869 | 0.8063792 | 0.65024741 | 5.84391381 | 0.80983106 | 0.65582635 | 5.77020127 |
| W Milford 2.5 | 0.80121949 | 0.64195267 | 6.20284431 | 0.79959719 | 0.63935567 | 6.20451294 | 0.80336245 | 0.64539122 | 6.05530595 |
| W Milford 3.2 | 0.80351101 | 0.64562994 | 6.00859581 | 0.80204849 | 0.64328177 | 6.00107739 | 0.80579841 | 0.64931107 | 5.88496121 |
| W Milford 5.5 | 0.8047245 | 0.64758152 | 6.00304217 | 0.80321088 | 0.64514772 | 5.99379891 | 0.80699555 | 0.65124182 | 5.88031498 |

| Tmax Statistics | | | | | | | | | |
|---------------------|-------------|----------------|------------|------------|----------------|------------|------------|----------------|------------|
| location | bcc-csm1-1m | | | CCSM4 | | | MRI-CGCM3 | | |
| | r | R ² | RMSE | r | R ² | RMSE | r | R ² | RMSE |
| Bloomingdale | 0.79944338 | 0.63910971 | 6.58983921 | 0.79586835 | 0.63340642 | 6.63262978 | 0.80502786 | 0.64806986 | 6.44356599 |
| Greenwood Lake | 0.80007418 | 0.6401187 | 6.59876692 | 0.79672544 | 0.63477143 | 6.63679674 | 0.8054719 | 0.64878498 | 6.45041295 |
| Ringwood 1.0 | 0.80045856 | 0.64073391 | 6.59425474 | 0.79690364 | 0.63505541 | 6.63913035 | 0.80561494 | 0.64901543 | 6.44658468 |
| Ringwood 3.0 | 0.79959032 | 0.63934468 | 6.60722344 | 0.79597092 | 0.63356971 | 6.65441241 | 0.80490888 | 0.64787831 | 6.45479076 |
| Ringwood | 0.79954365 | 0.63927006 | 6.61790217 | 0.79602147 | 0.63365018 | 6.66472875 | 0.80483041 | 0.647752 | 6.46070853 |
| Wanaque 0.6 | 0.79824569 | 0.63719618 | 6.61240617 | 0.79476235 | 0.6316472 | 6.65345137 | 0.80391852 | 0.64628499 | 6.46677241 |
| Wanaque Raymond Dam | 0.79891275 | 0.63826158 | 6.60361061 | 0.79544451 | 0.63273197 | 6.6406597 | 0.80438992 | 0.64704314 | 6.46816916 |
| W Milford 2.5 | 0.80172086 | 0.64275633 | 6.59239771 | 0.79827725 | 0.63724657 | 6.62477339 | 0.80704654 | 0.65132412 | 6.46084215 |
| W Milford 3.2 | 0.80071764 | 0.64114874 | 6.59049141 | 0.79741695 | 0.63587379 | 6.62248866 | 0.80604715 | 0.64971201 | 6.45185035 |
| W Milford 5.5 | 0.8026919 | 0.64431429 | 6.58163137 | 0.79935259 | 0.63896457 | 6.61362209 | 0.80768557 | 0.65235597 | 6.44867912 |

Table 4 – Calculated statistics (R, R², and Root Mean Square Error values) for the different locations chosen. Highlighted values show the best R² values (closest to 1).

| | | | |
|-------|----------------|----|--------------|
| Stats | BCC-CSM1-1m | r | -0.007895344 |
| | | r2 | 6.234E-05 |
| | MRI-CGCM3 | r | 0.037743309 |
| | | r2 | 1.4246E-03 |
| | CCSM4 | r | -0.041346779 |
| | | r2 | 1.7096E-03 |
| | bcc-csm1-1 | r | 0.091165507 |
| | | r2 | 8.3111E-03 |
| | BNU-ESM | r | 0.088645513 |
| | | r2 | 7.8580E-03 |
| | CanESM2 | r | 0.12785951 |
| | | r2 | 1.6348E-02 |
| | MIROC-ESM | r | 0.075748131 |
| | | r2 | 5.7378E-03 |
| | MIROC-ESM-CHEM | r | -0.059358204 |
| | | r2 | 3.5234E-03 |

Table 5– Statistics of monthly precipitation between 8 MACA models and PRISM for precipitation at Bloomington, 1981-2005. Highlighted value represents value closest to 1.

One study, evaluation and downscaling of CMIP5 climate simulations for the Southeast US by Mote et. Al (2015), previously referenced in Section 1.1, found that of 41 CMIP5 Global Climate Models (GCM)—including CCSM4, bcc-csm1-1m, and MRI-CGCM3—bcc-csm1-1m were consistently high in error, earning a high normalized error score of 0.9/1.0 and placing at 40 of 41 GCMs (Mote, et al., 2015). In the same report, CCSM4 earned the highest score at 18/41 with a normalized error score of approximately 0.3. Despite other authors finding the error of CCSM4 to be quite low, this study found CCSM4 to have extremely low correlation.

Mote, et al. (2015) also found that another MACA model from the 41 ranked GCM models, CNRM-CM5, ranked at 8th in terms of normalized error score. We correlated the output from this model against the PRISM.

| | | |
|----------|----|-------------|
| CNRM-CM5 | r | 0.109449424 |
| | r2 | 0.011979176 |

Table 6 – Correlation of MACA model CNRM-CM5 with PRISM in Bloomington

Though the R^2 value (Bloomingdale) is still quite low, there is a 191% increase in accuracy compared to the lowest value from the first attempt, which was the bcc-csm1-1m value of 6.23e-5. The CNRM-CM5 model provides the closest R^2 value to 1.

In a different study focusing on the Colombia River Basin (CRB) located mostly in Washington State, Idaho, and Oregon (partially in Canada, Montana, and Wyoming), researchers used MACA to look at precipitation seasonality and timing (Demirel & Moradkhani, 2015). Based on their research, which showed positive benefits in using MACA, we tested our MACA models on a location in the CRB. To easily access information, we decided on Portland, Oregon, and tested the coordinates of the Hayden Island Rain Gauge on bcc-csm1-1m, CCSM4, and MRI-CGCM3 (see Table 7 – Statistics for the Hayden Island Rain Gauge). We also checked if the interpolated values for Prism made any difference in comparison to the non-interpolated values, as our original values were non-interpolated.

| Precipitation Statistics | | | | | | | | | | | | |
|---|--------------|-----------|-----------|--------------|-----------|-----------|----------------|-----------|-----------|-----------------------------|-----------|-----------|
| Location | BCC vs Prism | | | MRI vs Prism | | | CCSM4 vs Prism | | | Prism Interpolated vs Prism | | |
| | r | r2 | RMSE | r | r2 | RMSE | r | r2 | RMSE | r | r2 | RMSE |
| General Portland | 0.5591487 | 0.3126472 | 2.2851453 | 0.5578179 | 0.3111608 | 2.3123879 | 0.5853684 | 0.3426562 | 2.2092171 | | | |
| Portland - Hayden Island Rain Gauge, Interpolated | 0.5369202 | 0.2882833 | 2.0751414 | 0.5709477 | 0.3259813 | 1.9851022 | 0.5536782 | 0.3065596 | 2.0488011 | | | |
| Portland - Hayden Island Rain Gauge, Not Interpolated | 0.5355751 | 0.2868407 | 2.0704472 | 0.5536476 | 0.3065257 | 2.0417461 | 0.5706363 | 0.3256258 | 1.9787349 | 0.9999193 | 0.9998387 | 0.0382525 |

| Tmin Statistics | | | | | | | | | | | | |
|---|--------------|-----------|-----------|--------------|-----------|-----------|----------------|-----------|-----------|-----------------------------|-----------|-----------|
| Location | BCC vs Prism | | | MRI vs Prism | | | CCSM4 vs Prism | | | Prism Interpolated vs Prism | | |
| | r | r2 | RMSE | r | r2 | RMSE | r | r2 | RMSE | r | r2 | RMSE |
| General Portland | 0.9141593 | 0.8356872 | 4.3640253 | 0.9158287 | 0.8387422 | 4.1473507 | 0.9028279 | 0.8150982 | 4.4378160 | | | |
| Portland - Hayden Island Rain Gauge, Interpolated | 0.9168271 | 0.8405720 | 3.5206406 | 0.9042249 | 0.8176227 | 3.3809369 | 0.9042249 | 0.8176227 | 3.6862388 | | | |
| Portland - Hayden Island Rain Gauge, Not Interpolated | 0.9164840 | 0.8399429 | 3.5139032 | 0.9172341 | 0.8413184 | 3.3739691 | 0.9038764 | 0.8169925 | 3.6802646 | 0.9999919 | 0.9999838 | 0.0444375 |

| Tmax Stats | | | | | | | | | | | | |
|---|--------------|-----------|-----------|--------------|-----------|-----------|----------------|-----------|-----------|-----------------------------|-----------|-----------|
| Location | BCC vs Prism | | | MRI vs Prism | | | CCSM4 vs Prism | | | Prism Interpolated vs Prism | | |
| | r | r2 | RMSE | r | r2 | RMSE | r | r2 | RMSE | r | r2 | RMSE |
| General Portland | 0.9447246 | 0.8925047 | 4.1784124 | 0.9473587 | 0.8974885 | 4.0356169 | 0.9480225 | 0.8987466 | 4.0047392 | | | |
| Portland - Hayden Island Rain Gauge, Interpolated | 0.9447565 | 0.8925649 | 4.2139067 | 0.9480354 | 0.8987710 | 4.0245327 | 0.9473454 | 0.8974633 | 4.0432142 | | | |
| Portland - Hayden Island Rain Gauge, Not Interpolated | 0.9447764 | 0.8926025 | 4.2119510 | 0.9473270 | 0.8974285 | 4.0447542 | 0.9481283 | 0.8989472 | 4.0212331 | 0.9999972 | 0.9999944 | 0.0371948 |

Table 7 – Statistics for the Hayden Island Rain Gauge

In comparison to the results from the Passaic River Basin, precipitation R^2 values were 97% more accurate—despite still only being 0.325 at the highest value. R^2 values for minimum

and maximum temperature were lower; for the Passaic River Basin, temperature R^2 values averaged 0.93 whereas CRB R^2 values averaged 0.84 for minimum temperature and 0.89 for maximum temperature.

There was an insignificant difference between the interpolated and non-interpolated PRISM values in Portland; however, the slight difference warranted a venture into re-downloading original PRISM values for the Passaic River Basin. We downloaded interpolated values for Bloomingdale (see Table 8 – Statistics for the interpolated PRISM values against bcc-csm1-1m, MRI-CGCM3, and CCSM4).

| Stats | | | | | | | | |
|---------------------------|-----------|-----------|---------------------------|-----------|-----------|-----------------------------|-----------|-----------|
| BCC vs Interpolated Prism | | | MRI vs Interpolated Prism | | | CCSM4 vs Interpolated Prism | | |
| r | r2 | RMSE | r | r2 | RMSE | r | r2 | RMSE |
| -0.0087606 | 0.0000767 | 2.6760948 | 0.0342519 | 0.0011732 | 2.4332190 | -0.0394837 | 0.0015590 | 2.6693973 |

Table 8 – Statistics for the interpolated PRISM values against bcc-csm1-1m, MRI-CGCM3, and CCSM4

With the R^2 values still significantly low, the interpolated values showed no distinct improvement versus non-interpolated.

3.2 Bias Correcting Historical Data

Because of the low correlation between the models and the PRISM precipitation values, it was imperative to bias-correct the data and determine whether or not the bias-correction methods chosen were effective.

3.2.1 Precipitation

The first method used in precipitation correction was the correction factor method. By taking the ratio of the monthly average PRISM to MACA precipitation and applying it to daily values within that month, precipitation values could be corrected in a simple, linear way. However, these linear corrections did not provide any significant improvement (see Table 9 – Daily Corrected Correlations).

| DAILY CF Corrected Maca and PRISM Correlations | | | | | | |
|--|---------------------|---------------|-------------------|---------------------|---------------|-------------------|
| | R | | | R2 | | |
| Location | PRISM v bcc-csm1-1m | PRISM v CCSM4 | PRISM v MRI-CGCM3 | PRISM v bcc-csm1-1m | PRISM v CCSM4 | PRISM v MRI-CGCM3 |
| Bloomingtondale | 0.017190051 | -0.016836623 | -0.013210881 | 0.000295498 | 0.000283472 | 0.000174527 |
| Greenwood Lake | 0.020551929 | -0.019782585 | -0.011526613 | 0.000422382 | 0.000391351 | 0.000132863 |
| Ringwood 1.0 | 0.023557933 | -0.015825998 | -0.011340434 | 0.000554976 | 0.000250462 | 0.000128605 |
| Ringwood 3.0 | 0.02033071 | -0.018362264 | -0.018362264 | 0.000413338 | 0.000337173 | 0.000337173 |
| Ringwood | 0.020378278 | -0.017342248 | -0.013409128 | 0.000415274 | 0.000300754 | 0.000179805 |
| Wanaque 0.6 S | 0.013774404 | -0.016928988 | -0.018018741 | 0.000189734 | 0.000286591 | 0.000324675 |
| Wanaque Raymond Dam | 0.020128192 | -0.004112498 | -0.01169786 | 0.000405144 | 1.69126E-05 | 0.00013684 |
| W Milford 2.5 SSE | 0.017522988 | -0.019166587 | -0.013183437 | 0.000307055 | 0.000367358 | 0.000173803 |
| W Milford 3.2 NE | 0.021137605 | -0.019979091 | -0.011572626 | 0.000446798 | 0.000399164 | 0.000133926 |
| W Milford 5.5 NE | 0.022204562 | -0.018224861 | -0.011460412 | 0.000493043 | 0.000332146 | 0.000131341 |

Table 9 – Daily Corrected Correlations

Comparing these values to the uncorrected, there is little improvement in the precipitation correlation coefficient:

| Correlations between raw and correction-factor MACA precipitation | | | | | | |
|---|---------------------|---------------|-------------------|---------------------|---------------|-------------------|
| | Raw | | | CF | | |
| Location | PRISM v bcc-csm1-1m | PRISM v CCSM4 | PRISM v MRI-CGCM3 | PRISM v bcc-csm1-1m | PRISM v CCSM4 | PRISM v MRI-CGCM3 |
| Bloomingtondale | -0.007895344 | -0.041346779 | 0.037743309 | 0.017190051 | -0.016836623 | -0.013210881 |
| Greenwood Lake | 0.004527278 | -0.09140164 | 0.028032977 | 0.020551929 | -0.019782585 | -0.011526613 |
| Ringwood 1.0 | 0.022049835 | -0.063343943 | 0.046824866 | 0.023557933 | -0.015825998 | -0.011340434 |
| Ringwood 3.0 | 0.013987827 | -0.062674619 | 0.045596558 | 0.02033071 | -0.018362264 | -0.018362264 |
| Ringwood | 0.005831563 | -0.056417696 | 0.046988655 | 0.020378278 | -0.017342248 | -0.013409128 |
| Wanaque 0.6 S | -0.012191279 | -0.035970264 | 0.040128752 | 0.013774404 | -0.016928988 | -0.018018741 |
| Wanaque Raymond Dam | -0.005617157 | -0.037120478 | 0.037940448 | 0.020128192 | -0.004112498 | -0.01169786 |
| W Milford 2.5 SSE | -0.010610954 | -0.070449475 | 0.014499061 | 0.017522988 | -0.019166587 | -0.013183437 |
| W Milford 3.2 NE | 0.003513159 | -0.084300957 | 0.026701608 | 0.021137605 | -0.019979091 | -0.011572626 |
| W Milford 5.5 NE | -0.000166232 | -0.086457721 | 0.030086976 | 0.022204562 | -0.018224861 | -0.011460412 |

Table 10 – Correlation between raw MACA and corrected MACA precipitation

The percent change in correlation ranges from 8% to nearly 13,000%. Despite the enormous range in correlation percent change, the correlation coefficients themselves still remain incredibly low. As mentioned in Section 2.1.2, the MACA model is not intended to serve as a weather hindcast, likely partially explaining the low correlation in precipitation values. The correlation coefficient and coefficient of determination are not the only ways of validating data; therefore, another method of data verification was explored.

Several programs in R offer statistical analysis, but the qmap package specifically bias-corrects precipitation data. Qmap uses quantile mapping to bias-correct model output. However, the correlation between the bias-correction from qmap and PRISM is even lower than the correlations between the raw output and the correction factor (CF) data and PRISM (see Table 11).

| R | | |
|----------------|---------------|------------|
| Prism, raw_bcc | Prism, CF_bcc | Prism, R |
| -0.022724068 | -0.022724068 | -0.0189301 |

Table 11 – Correlations between raw bcc-csm1-1m, CF corrected bcc-csm1-1m, and qmap-corrected bcc-csm1-1m data to PRISM

Surprisingly, the correlation between PRISM and the qmap-corrected data was not just low but showed even less of a direct relationship between the datasets. Another approach towards validation was then required.

After seeing the low correlation coefficients, looking at the overall distribution became the next step in attempting to validate the results. At this point, it became important to look at the CDF of the models in comparison to each other and how they fit against PRISM (see Figure 5 – CDFs of each MACA model against PRISM). Though it is difficult to immediately identify whether MRI-CGCM3 or CCSM4 is more accurate, there is a clear distinction between PRISM and bcc-csm1-1m, which generally overestimates precipitation.

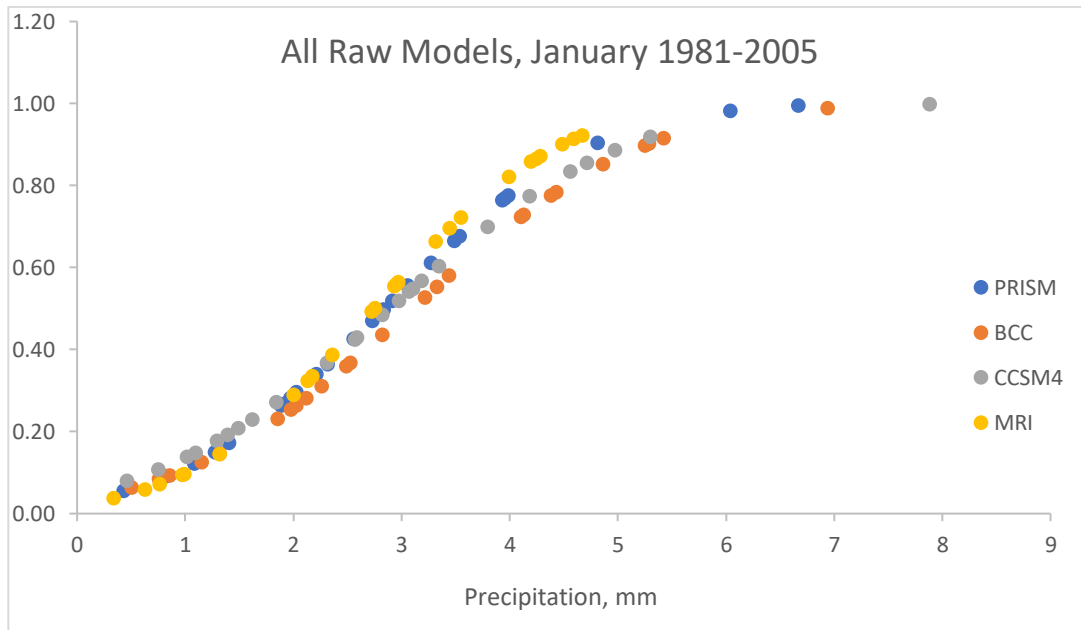
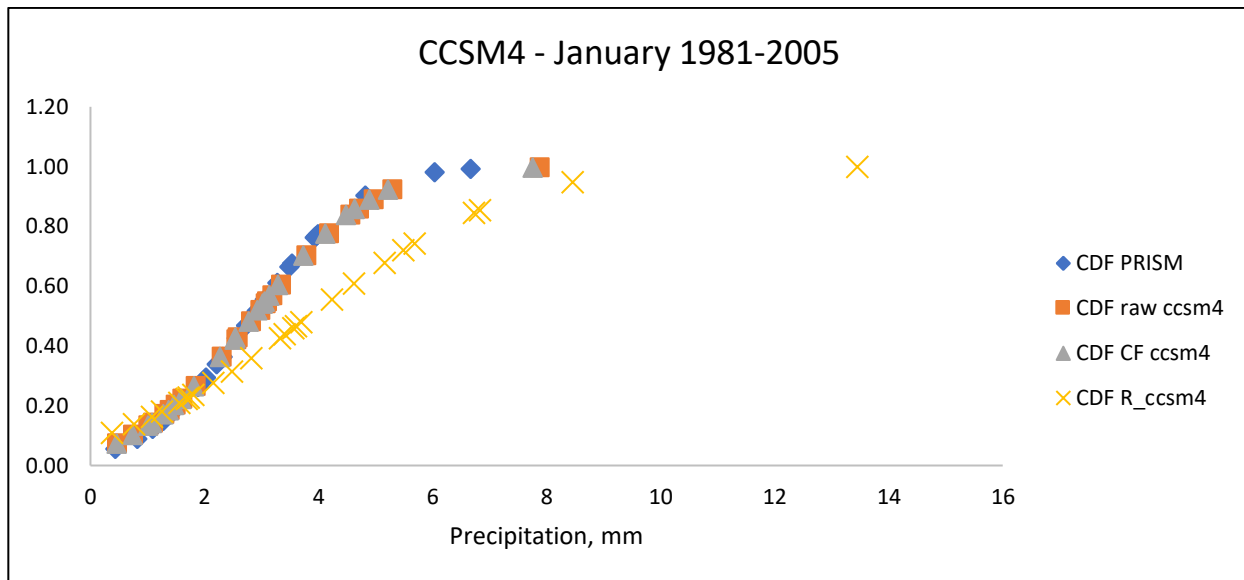
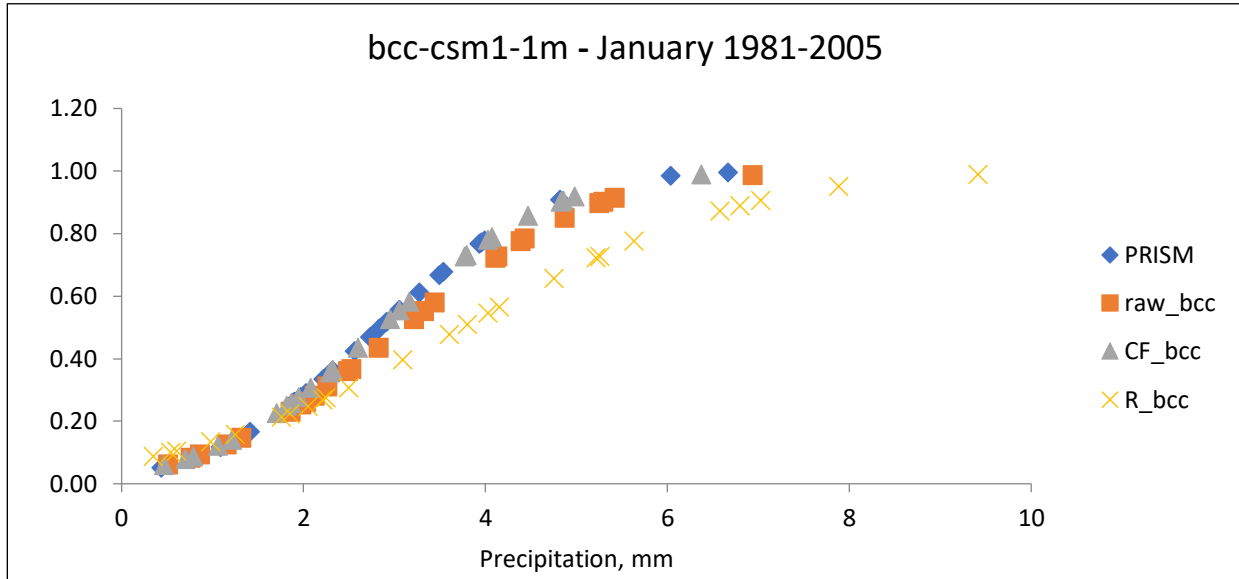


Figure 5 – CDFs of each MACA model against PRISM

CDFs of PRISM, CF MACA, raw MACA, and qmap MACA were then plotted and compared to each other for a fuller understanding of the cumulative distribution of data (see Figure 6 – CDFs of the raw data and corrected data against PRISM).



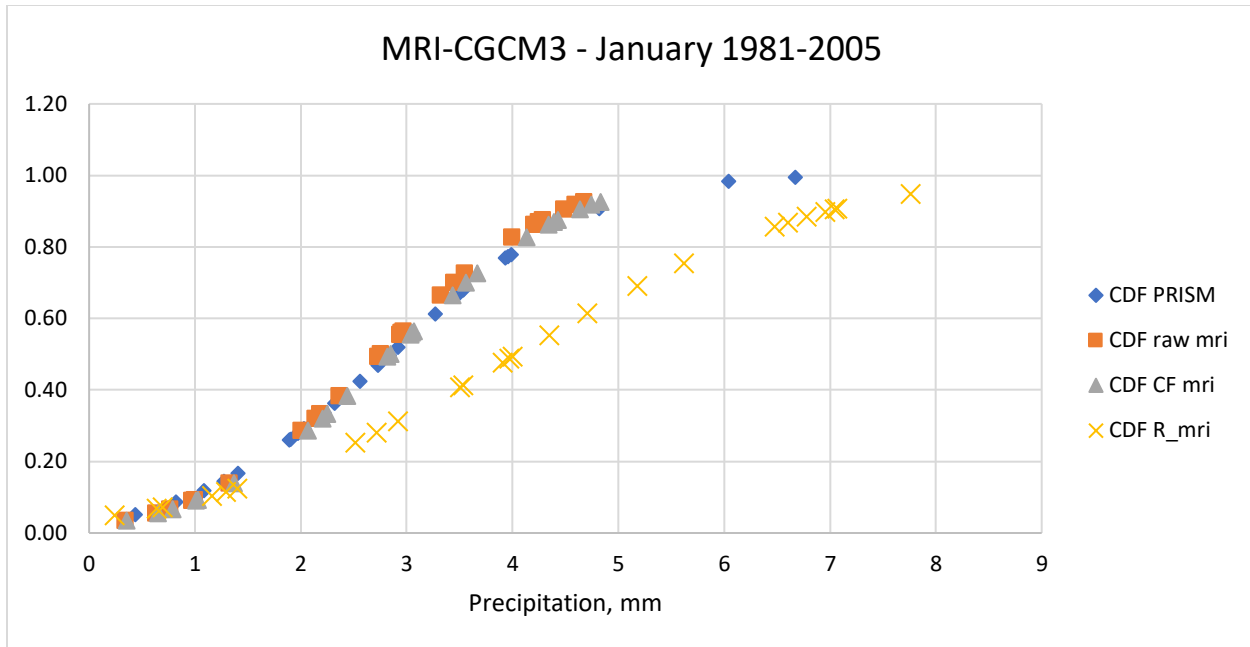
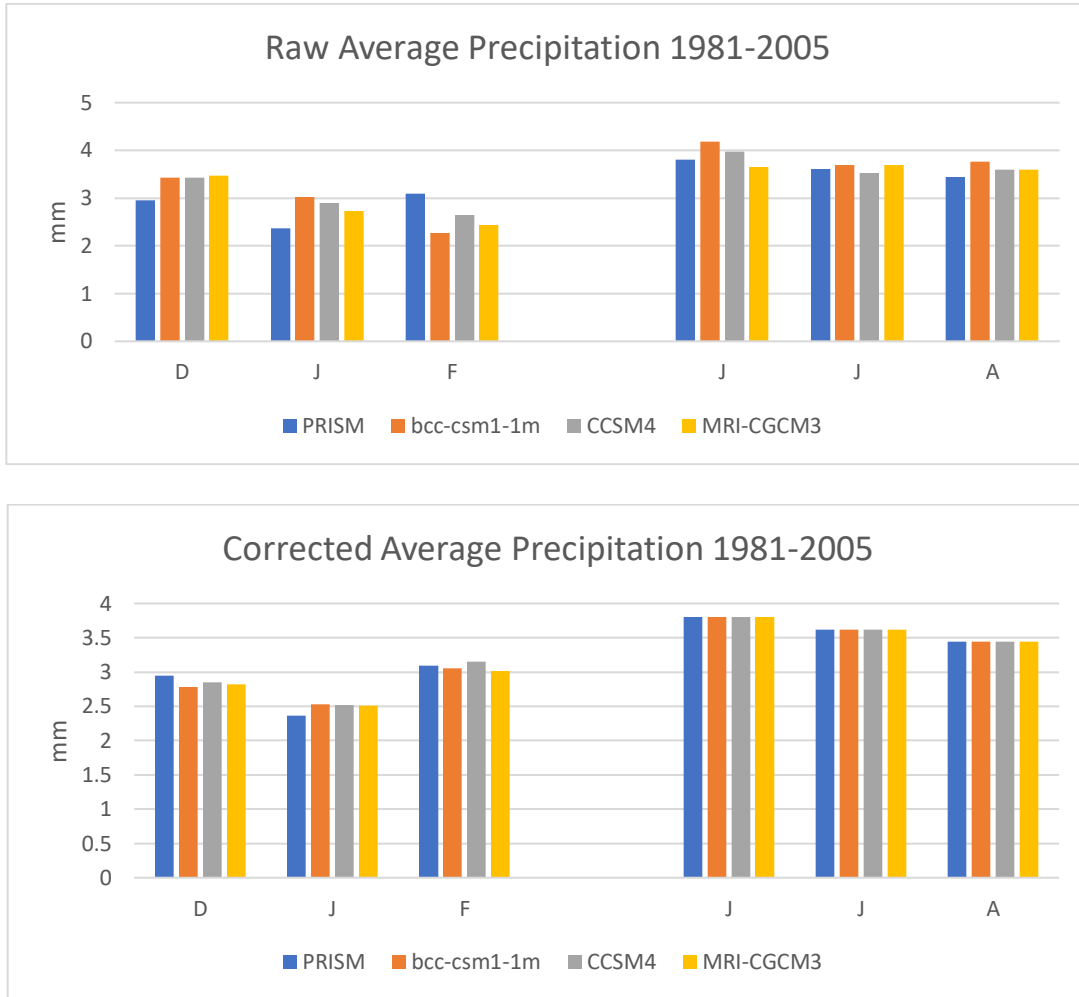


Figure 6 – CDFs of the raw data and corrected data against PRISM

From the CDFs in each model, it is clearly seen that though the distribution of the data corrected by the qmap package has a slightly different curve, the distribution of the raw and CF MACA data are almost exact replicas of each other. Also noteworthy is the improved CDF of the corrected MACA model to the raw model. Though the differences are slight between the respective models, the distribution of the correction-factor corrected CDF most closely matches that of the PRISM model.

Having seen the CDF of the corrected data as closer to the observed than the original, it was then decided to look at a snapshot of seasonal precipitation. New Jersey tends to experience more precipitation in the summer months of June, July, and August (JJA); therefore, comparing the precipitation from summer months to December, January, and February (DJF) seemed the next logical step to validate accuracy. In comparing the raw average precipitation for JJA and DJF against the corrected values for the respective months, there is a clear distinction between the two graphs (see Figure 7 – Comparison of seasonal average precipitation for winter and summer months). Raw model precipitation in particular shows disagreements between the models by month

for the winter months, whereas the summer months show more cohesive, united results. The models in general overestimate precipitation in comparison to the PRISM values. This may perhaps be attributed to the difficulty that GCMs have in capturing smaller, localized storm fronts.



| Correlation | r |
|-----------------|------------|
| Prism/raw bcc | 0.63259371 |
| Prism/raw CCSM4 | 0.73634863 |
| Prism/raw MRI | 0.68893687 |
| Prism/CF bcc | 0.97973767 |
| Prism/CF CCSM4 | 0.98885205 |
| Prism/CF mri | 0.98510118 |

Figure 7 – Comparison of seasonal average precipitation for winter and summer months with correlations

After correction, the monthly averages not only tend to match PRISM much more significantly, but they agree more amongst themselves. Looking at the corrected average

precipitation, the summer months are nearly identical to PRISM and the correlation coefficient reflects this, with values averaging 0.98. This is a drastic increase from the correlation coefficients for the 1981-2005 daily time series, which saw values as low as 0.000016. Therefore, although the daily time series for 25 years may not be significantly accurate, the accuracy at the monthly scale proves that MACA can be accurate in predicting seasonal-scale climate shifts.

3.2.2 Temperature

Temperature is not corrected through a multiplicative method. Instead, bias correction is performed through additive measures. Interestingly, although bias-correction helped improve precipitation, temperature bias-correction executed through the linear additive method actually decreased the correlation coefficient in a several cases (see **Error! Reference source not found.**).

| CF Tmax Statistics | | | | | | |
|--------------------|-------------|------------|------------|------------|------------|------------|
| location | bcc-csm1-1m | | CCSM4 | | MRI-CGCM3 | |
| | raw r | CF r | raw r | CF r | raw r | CF r |
| Bloomington | 0.79944338 | 0.79814605 | 0.79586835 | 0.79590347 | 0.80502786 | 0.80565878 |
| Ringwood | 0.79954365 | 0.79922243 | 0.79602147 | 0.79699099 | 0.80483041 | 0.80630154 |
| Wanaque 0.6 | 0.79824569 | 0.7971977 | 0.79476235 | 0.79503192 | 0.80391852 | 0.80478262 |
| W Milford 2.5 | 0.80172086 | 0.79840216 | 0.79827725 | 0.79621778 | 0.80704654 | 0.80572789 |
| W Milford 3.2 | 0.80071764 | 0.79857837 | 0.79741695 | 0.79663436 | 0.80604715 | 0.80587455 |
| W Milford 5.5 | 0.8026919 | 0.80046134 | 0.79935259 | 0.79848389 | 0.80768557 | 0.80741758 |

Table 12 - Statistics of corrected and uncorrected Tmin and Tmax

Because the correlations were either made worse or not significantly improved, the additive method was not considered a reliable method of temperature bias-correction. At correlations on average of 0.8, the daily time series for temperature was still statistically significant. Looking at the DJF and JJA seasonal averages also helped confirm that no further correction was necessary. The correlation between PRISM and the models for the summer and winter months was 0.99 for

both, Tmin and Tmax. As with precipitation, MACA performs better on the monthly scale over the daily. Despite the slightly lower correlation with daily temperature, raw MACA temperature values are considered satisfactory for the purposes of this study.

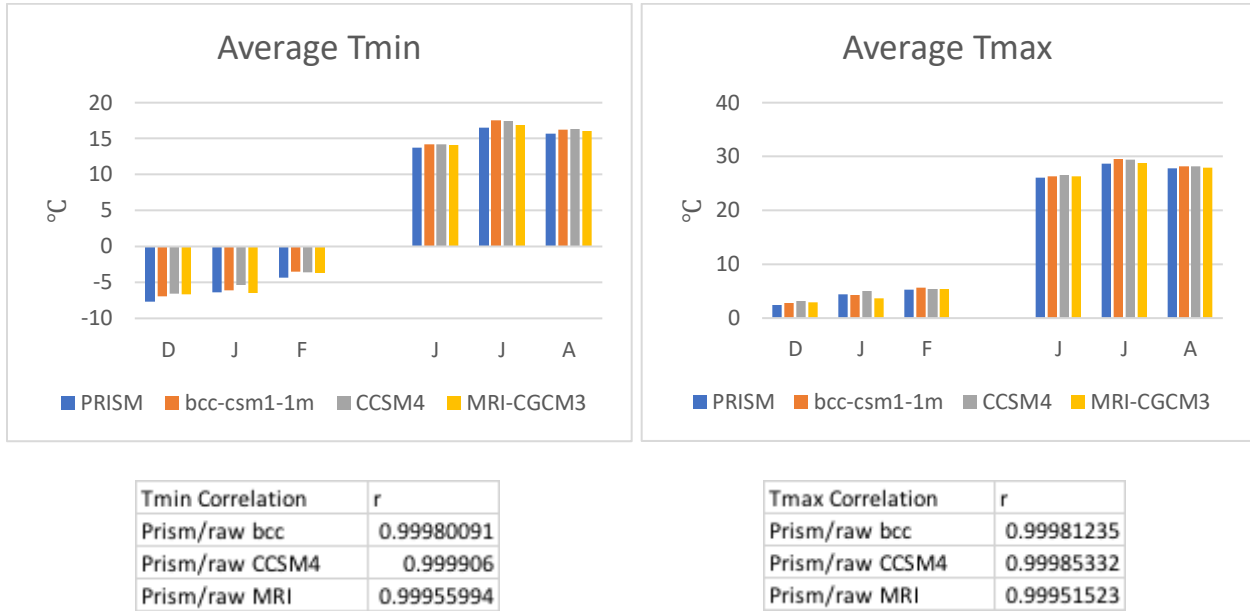


Figure 8 – Tmin, Tmax monthly comparison with correlation coefficient

3.2.3 Future 4.5 and 8.5 RCP

Based on the results from the historical data, it was decided while temperature would not be further corrected, the daily precipitation values in RCPs 4.5 and 8.5 would be corrected using the same correction factors per location by month as their historical counterparts.

3.3 Climatology

3.3.1 Historic Temperature

3.3.1.1 TN10p

Very cold nights, TN10p, represent the bottom 10th percentile of nightly temperatures. By looking at the historic trends in TN10p, a general established pattern can be compared to the future trends. Figure 9 shows the anomalies in the TN10p; by looking at the total difference from the average TN10p per year, a general trend can be defined. The trend of cold nights decreases from

1981 to 2005. Though the models disagree about exactly when the percentage cold nights decrease—PRISM, bcc-csm1-1m, and CCSM4 all mark this general downward trend turning point around 1994—they all show a decrease in total percentage of very cold nights.

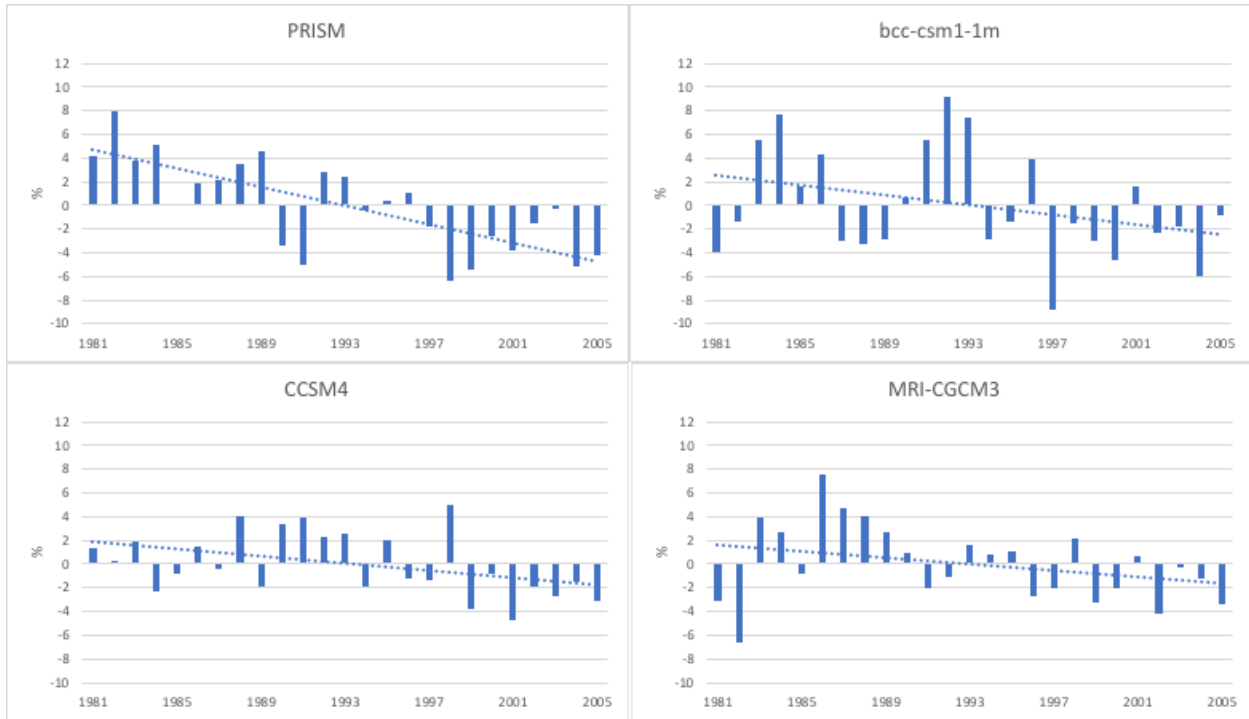


Figure 9 –Anomalies in coldest nights

3.3.1.2 TN90p

Very warm nights, TN90p, represent the 90th percentile of minimum temperatures. Figure 10 showing TN90p shows an overall increase in the anomalies for the warmest nights. Though there are a few dips in the moving average through the years, which may be partially attributed to the El Niño/La Niña phenomenon (Yun, et al., 2016), the overall trend shows an increase in percentage of days in which the minimum temperature is greater than 90% of total temperatures.

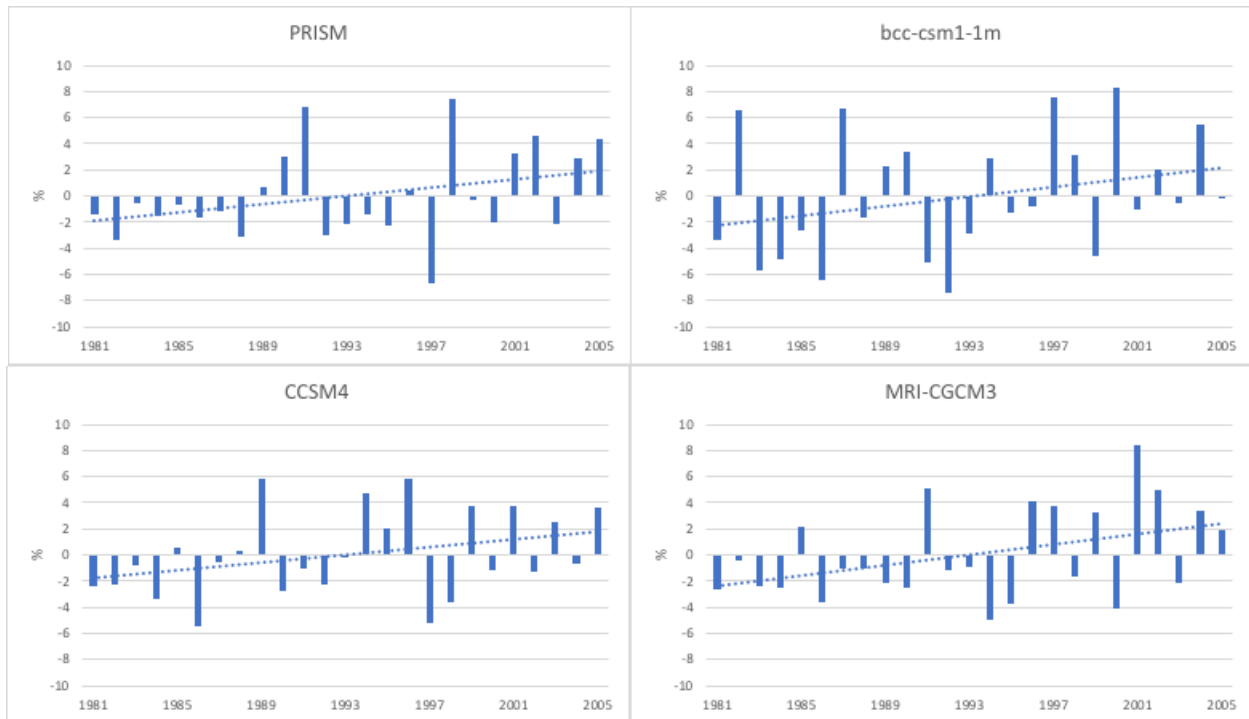


Figure 10 –Anomalies in the warmest nights

3.3.2 Precipitation and Droughts

3.3.2.1 CDD

Consecutive dry days (CDD) are the maximum count of days in which the precipitation is less than 1 mm. bcc-csm1-1m predicts a low number of consecutive dry days because of the overestimating of precipitation, which was clear in the cumulative distribution chart. The raw CDD anomalies seem to disagree about the maximum amount of dry days. The raw CCSM4 data, for example, predicts lower than average CDD until 1988, at which point the CDD skyrockets to nearly 28 days higher than the average. Bcc-csm1-1m predicts a similar pattern of lower than average CDD until 1993, after which point it continues to decrease until 2002. PRISM predicts wetter years from 1989 to 1998, after which point the dry days increase above the average. Despite the corrections made to daily data, it did not significantly impact the overall anomalies.

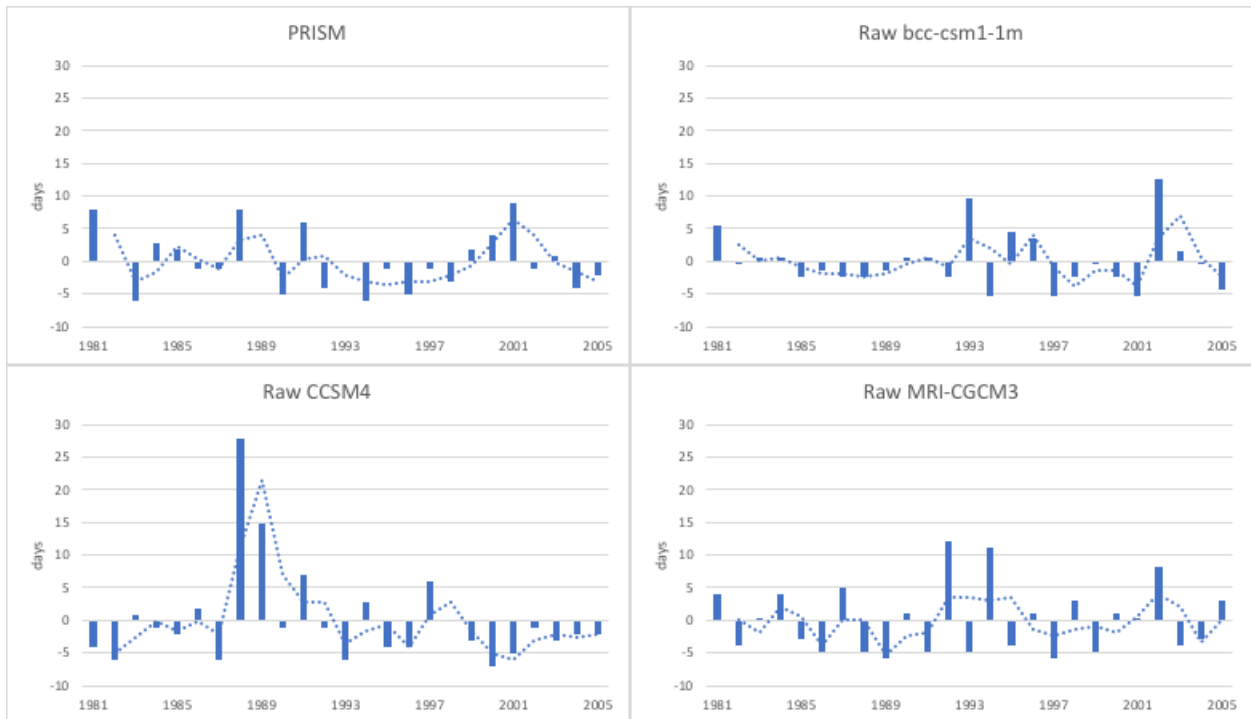


Figure 11 – Anomalies for raw consecutive dry days (CDD)

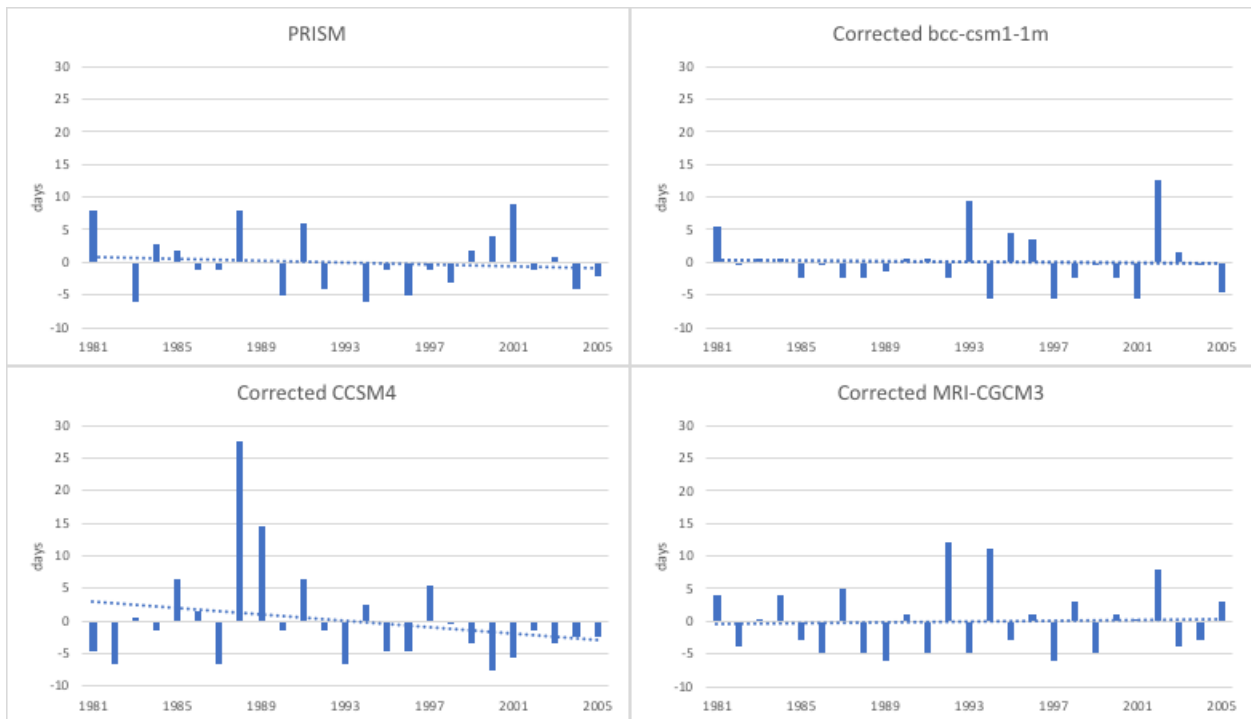


Figure 12 - Anomalies for bias-corrected consecutive dry days

The trends between the different models were also interesting to use as a source of comparison. The trend in consecutive dry days from CCSM4 most closely matches the PRISM trendline at a negative slope, while the trend line for bcc-csm1-1m is nearly neutral (see Figure

13). Surprisingly, the consecutive dry day trendline for MRI-CGCM3 shows that it is the only model amongst the other climate models to show a historical increase in CDD. Therefore, PRISM and CCSM4 agree that the average amount of days that consecutively have less than 1 mm of precipitation per year decrease over time; that is, the consecutive dry days decrease from 1981-2005.

As with the anomalies, the trend line for the corrected CDD is minimally impacted by the daily corrections (see Figure 14).

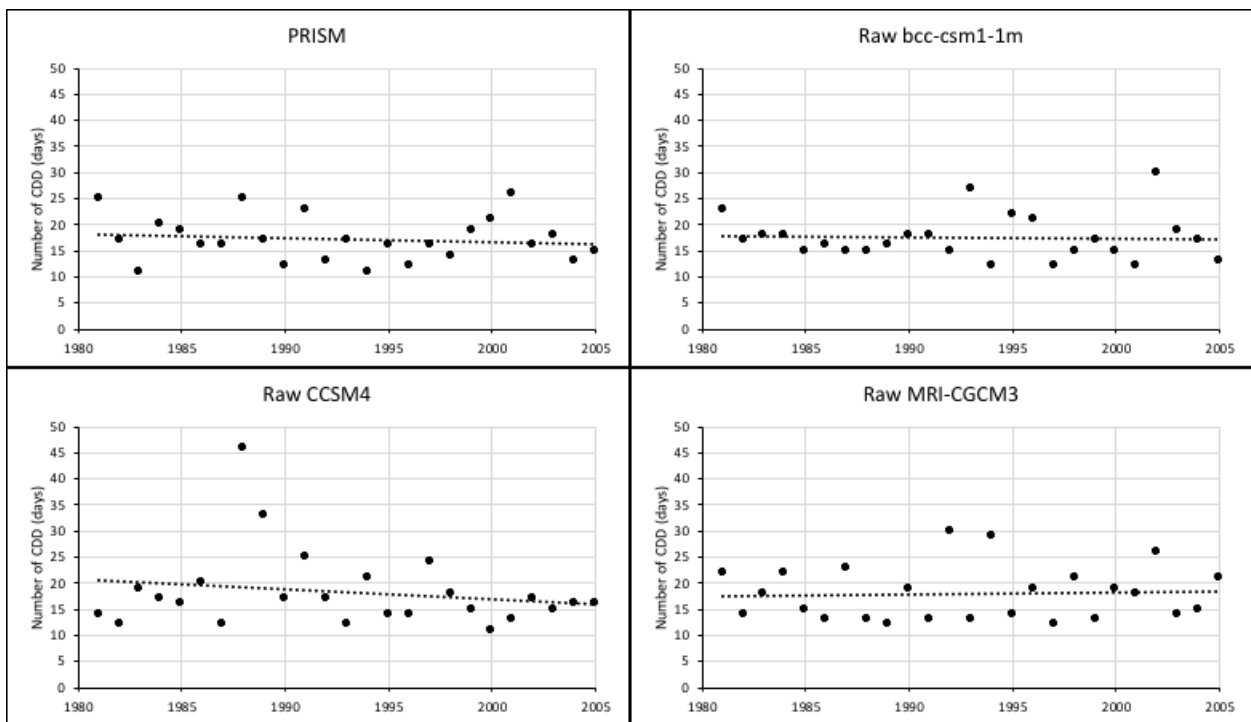


Figure 13 - CDD trends using raw data

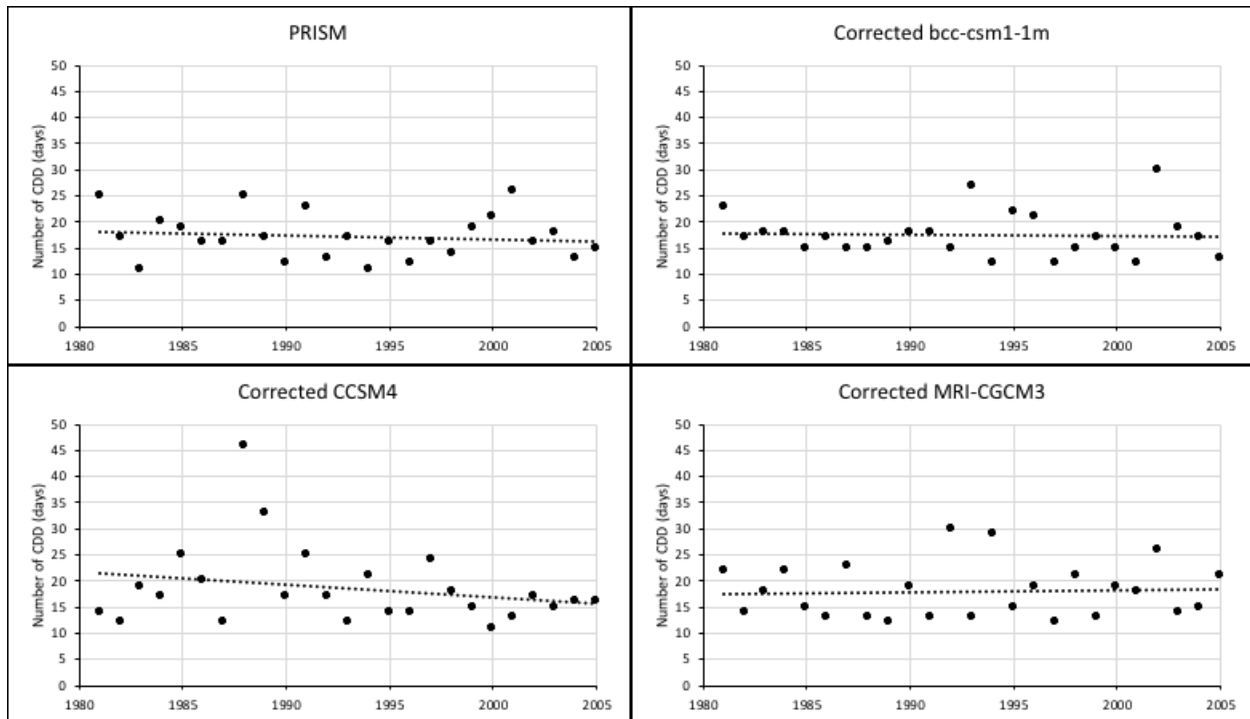


Figure 14- CDD trends using corrected data

3.3.2.2 R10

The count of days in which precipitation exceeds 10 mm is an extremely useful climatic index. If the amount of days in which 10 mm of precipitation falls increases, then it will consequently impact the indices accounting for extreme precipitation and maximum consecutive precipitation. Knowing the amount of rain or snow fall and the days over which the precipitation may occur affects several involved stakeholders in the general PRB community, such as those who live or otherwise maintain businesses in flood zones, architects and engineers, and agriculture specialists whose crop may be endangered.

The anomalies between the corrected and raw R10 are mostly mirrors of each other, with some differences by year. In 1985, for example, the raw CCSM4 model predicts 10 days less than the 1981-2005 average, whereas the corrected CCSM4 model predicts 7 days less than the baseline

average. Therefore, although the total amount by year may differ, the total running average trendline is not majorly affected. All models show a positive trend in R10.

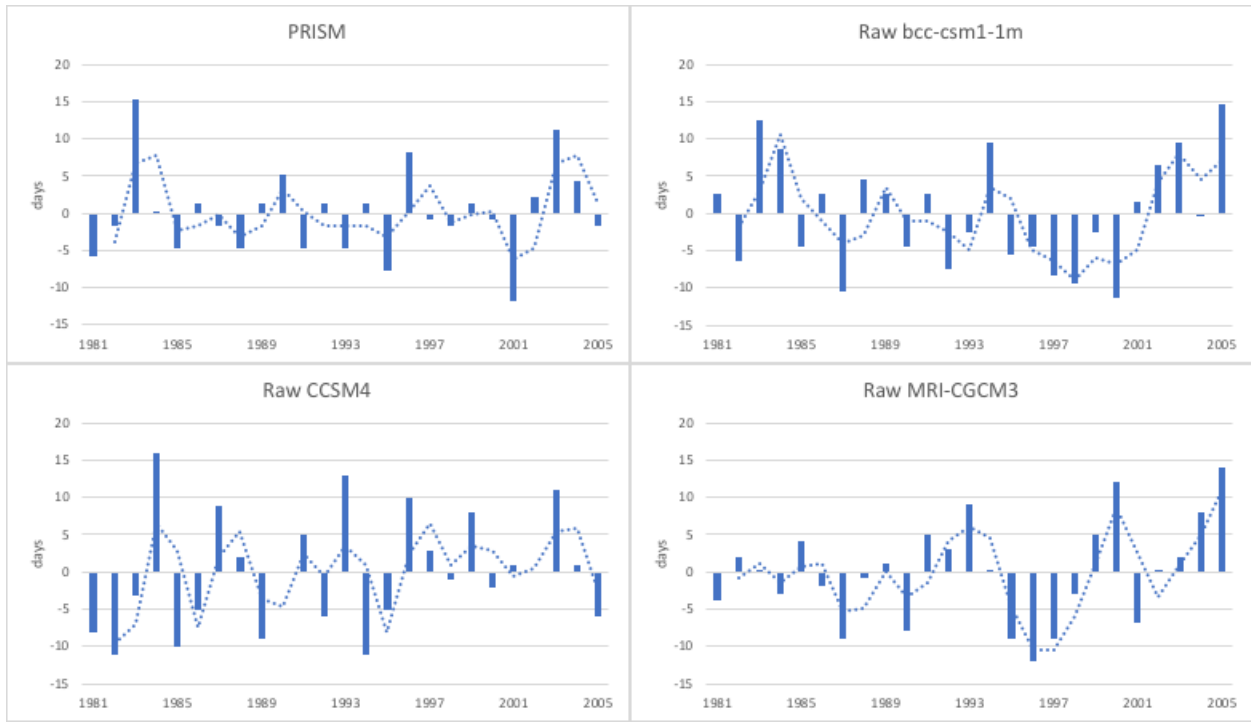


Figure 15 – Anomalies for raw wet days

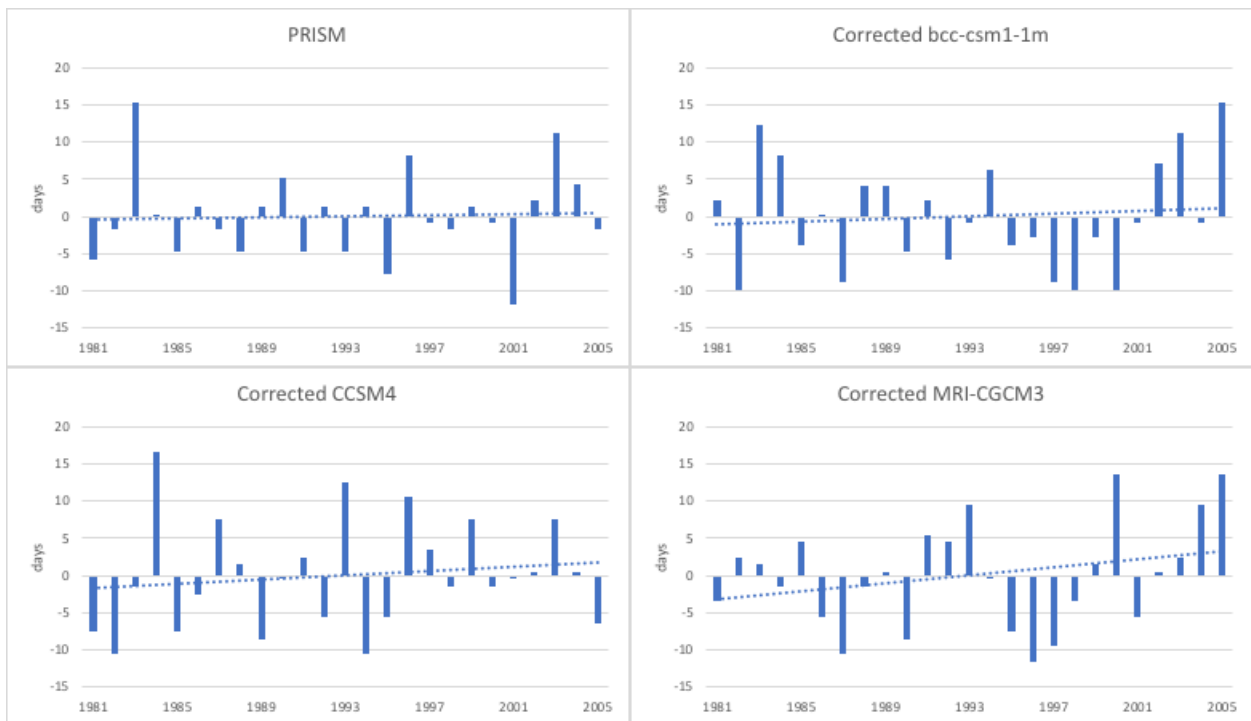


Figure 16 - Anomalies for corrected wet days

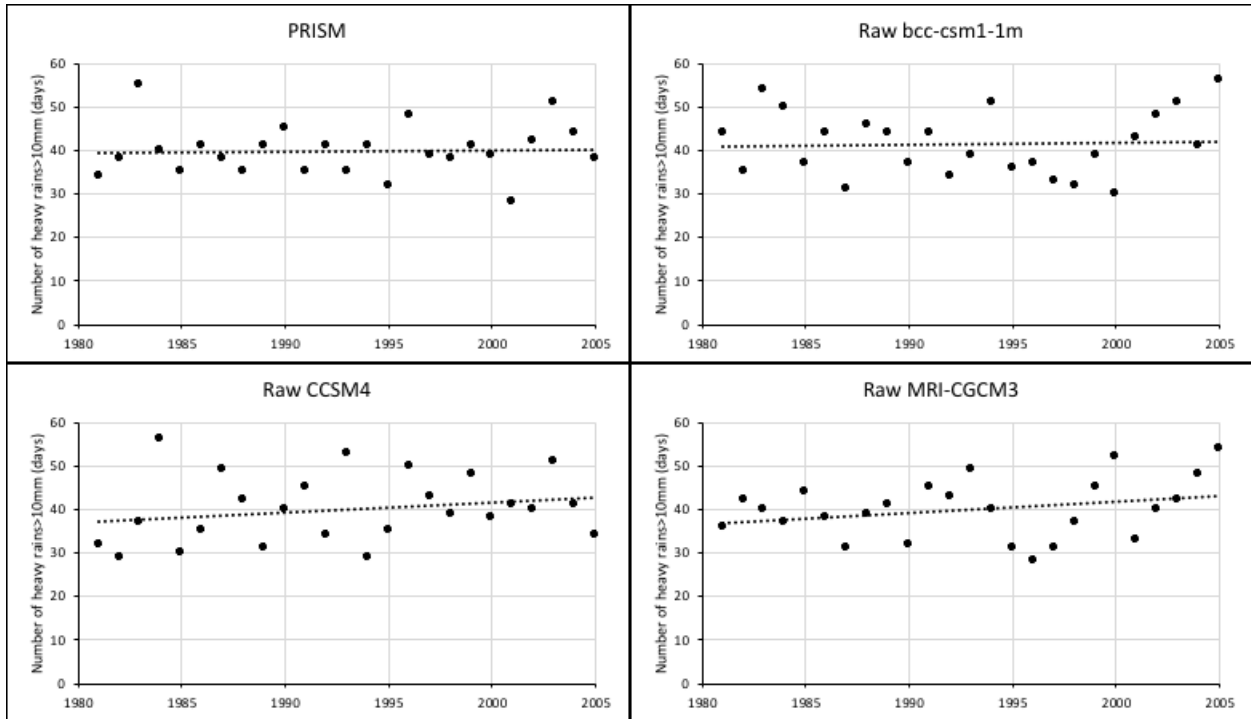


Figure 17 - R10 trends using raw data

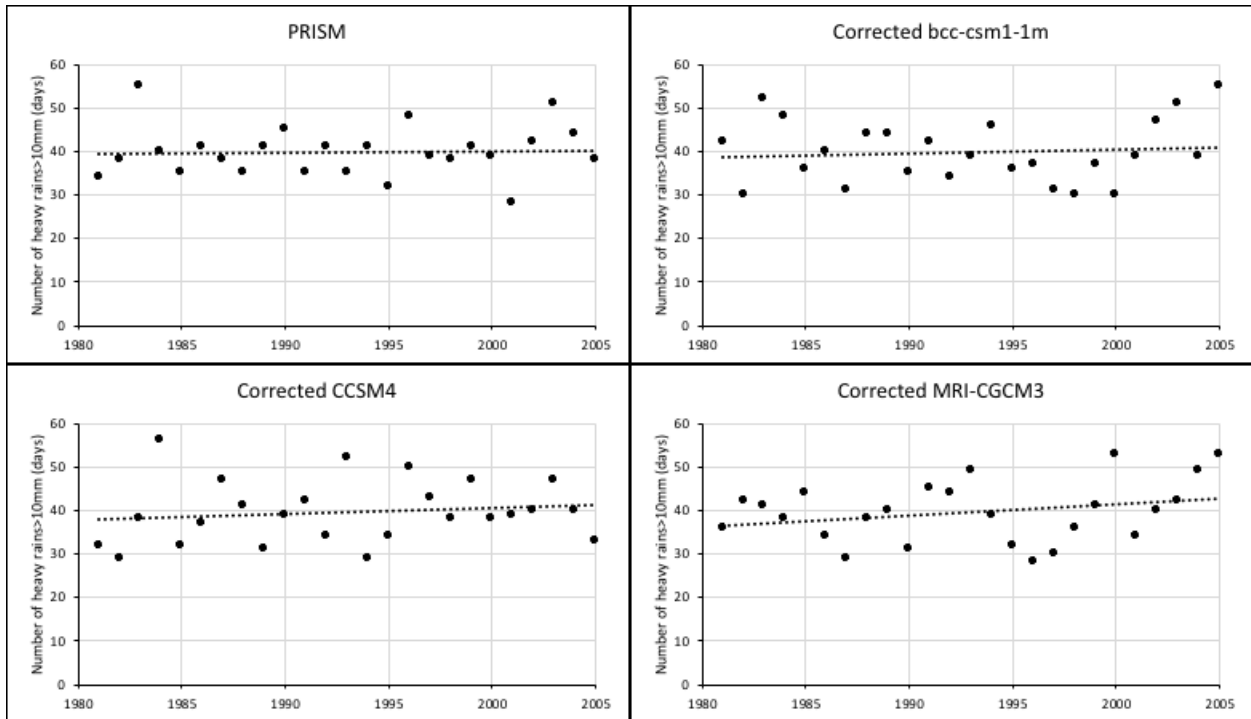


Figure 18 - R10 trends using corrected data

3.3.2.3 R95p

Extreme rainfall, R95p, represents the 95th percentile of precipitation. This information is incredibly important to analyze because heavy precipitation can lead to flooding, damaged

infrastructure, and loss of life. For R95p, the extremes in PRISM most closely match those of CCSM4. MRI-CGCM3 and bcc-csm1-1m both have extreme precipitation predictions on lower scales, whereas CCSM4 and PRISM have high precipitation values close to 300 mm above the average and low values near 200 below the average.

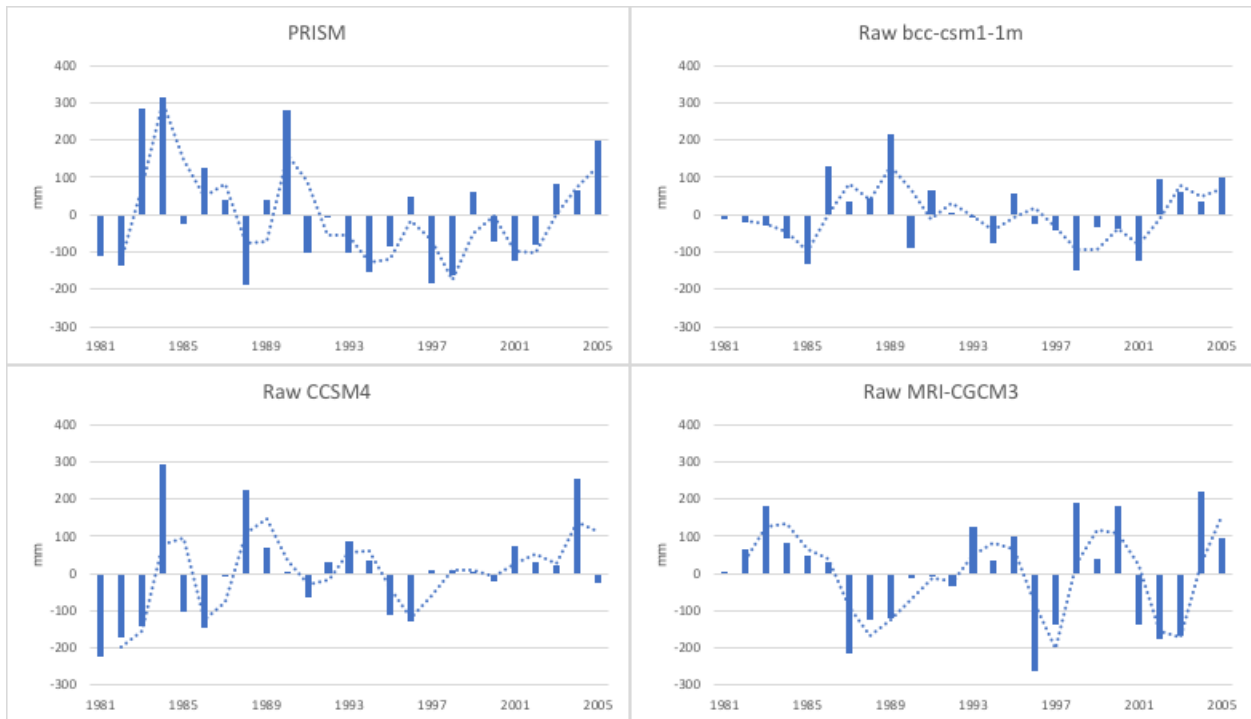


Figure 19 – Anomalies for raw extreme precipitation

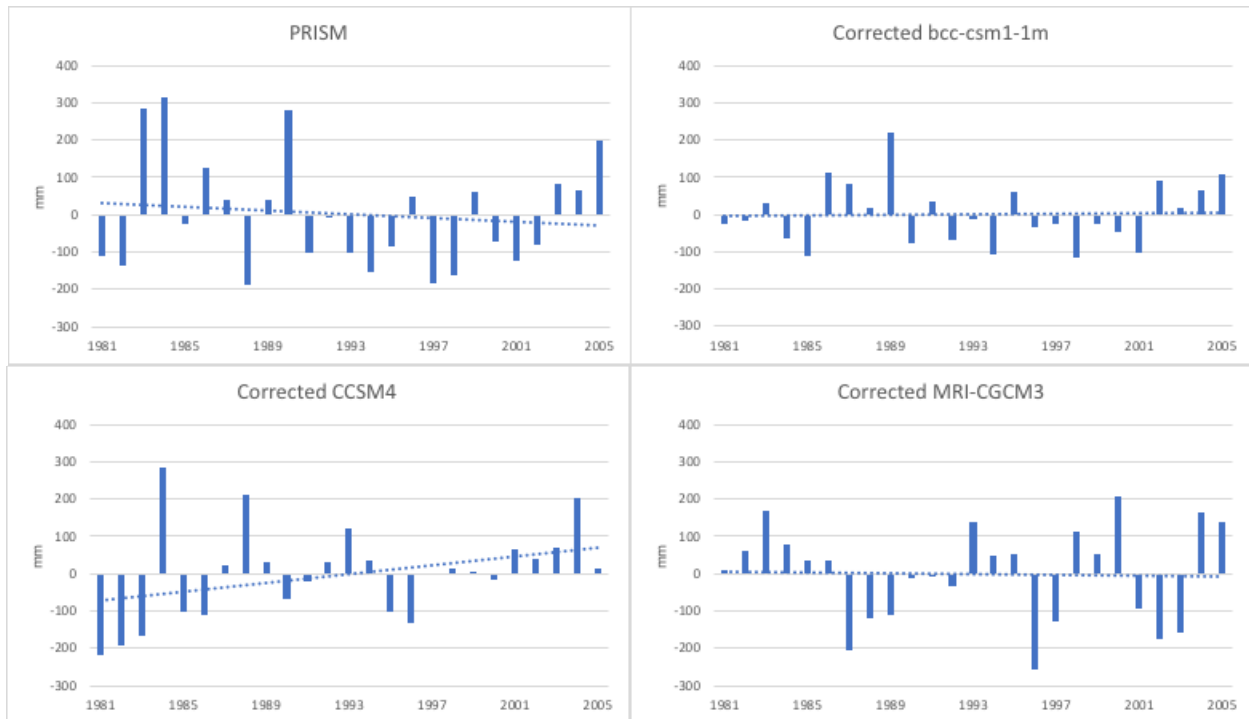


Figure 20 - Anomalies for corrected extreme precipitation

The trends are also varied amongst the different models. PRISM and the raw MRI-CGCM3 both show a decrease in the amount of precipitation in the 95th percentile, whereas bcc-csm1-1m and CCSM4 show an overall increasing trend. In this circumstance, the corrected data for CCSM4 makes a large difference. The trend line for the raw R95p CCSM4 data is at a significantly greater positive slope than the corrected data, which is closer to a more even 0 slope. In this instance, correction works well; even though the slope remains positive compared the negative PRISM slope, corrections allow for drastic changes in data to more closely match the observed.

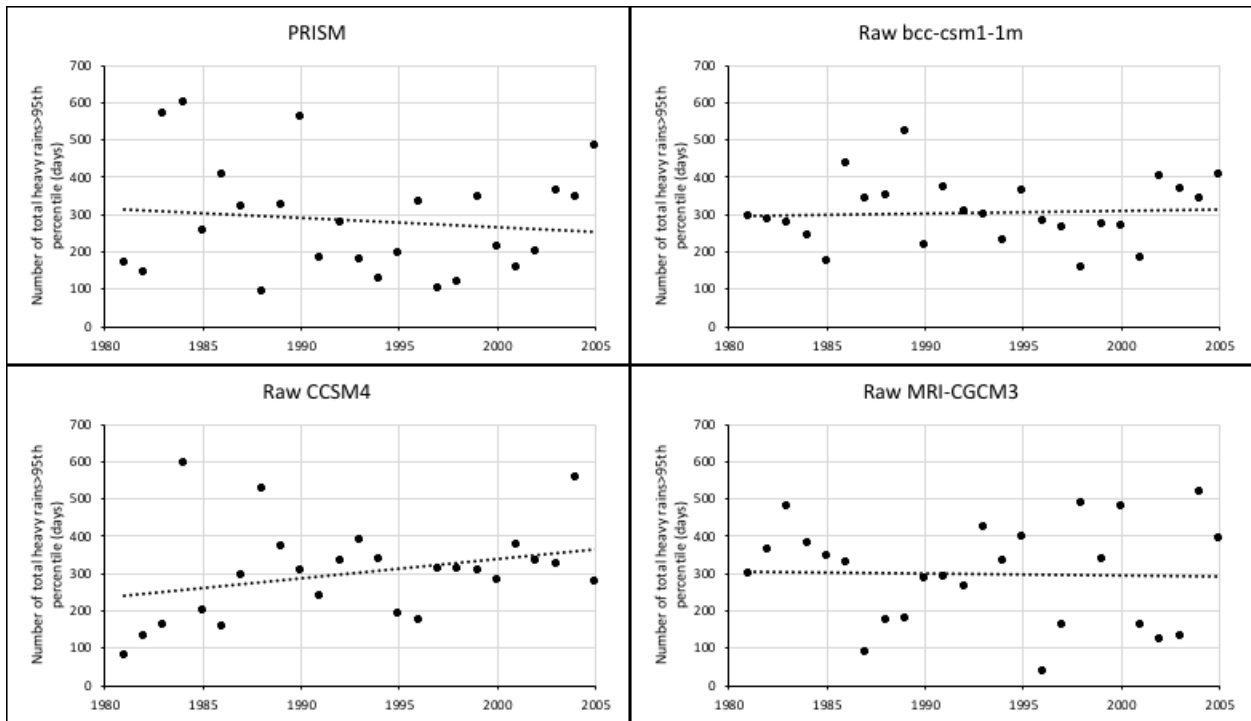


Figure 21- R95p trends using raw data

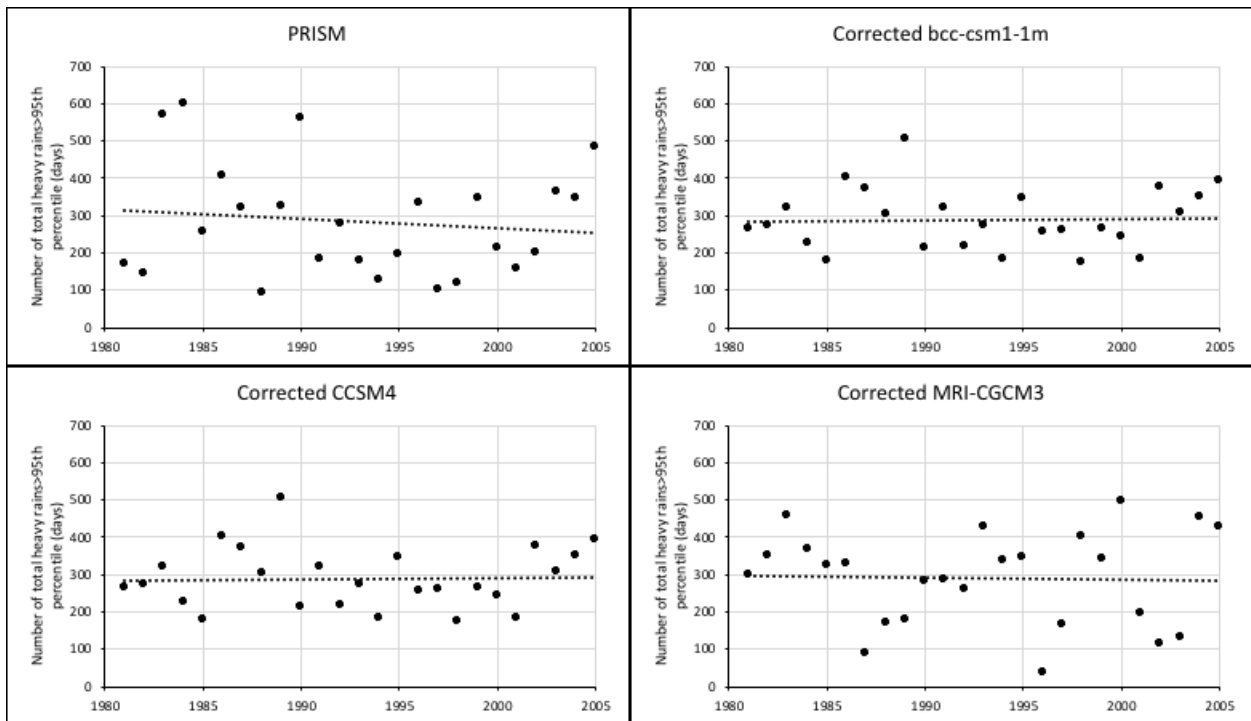


Figure 22- R95p trends using corrected data

3.3.2.4 R5xday

The yearly maximum consecutive 5-day precipitation, Rx5day, is the final climate marker analyzed in this study. Although the models disagree with the amount of yearly precipitation, there

is a correlation of 0.44 between the Rx5day for bcc-csm1-1m and PRISM. Compared to the others, which have correlations of -0.01 and -0.005 between CCSM4 and MRI-CGCM3 respectively, it is a significantly better relationship.

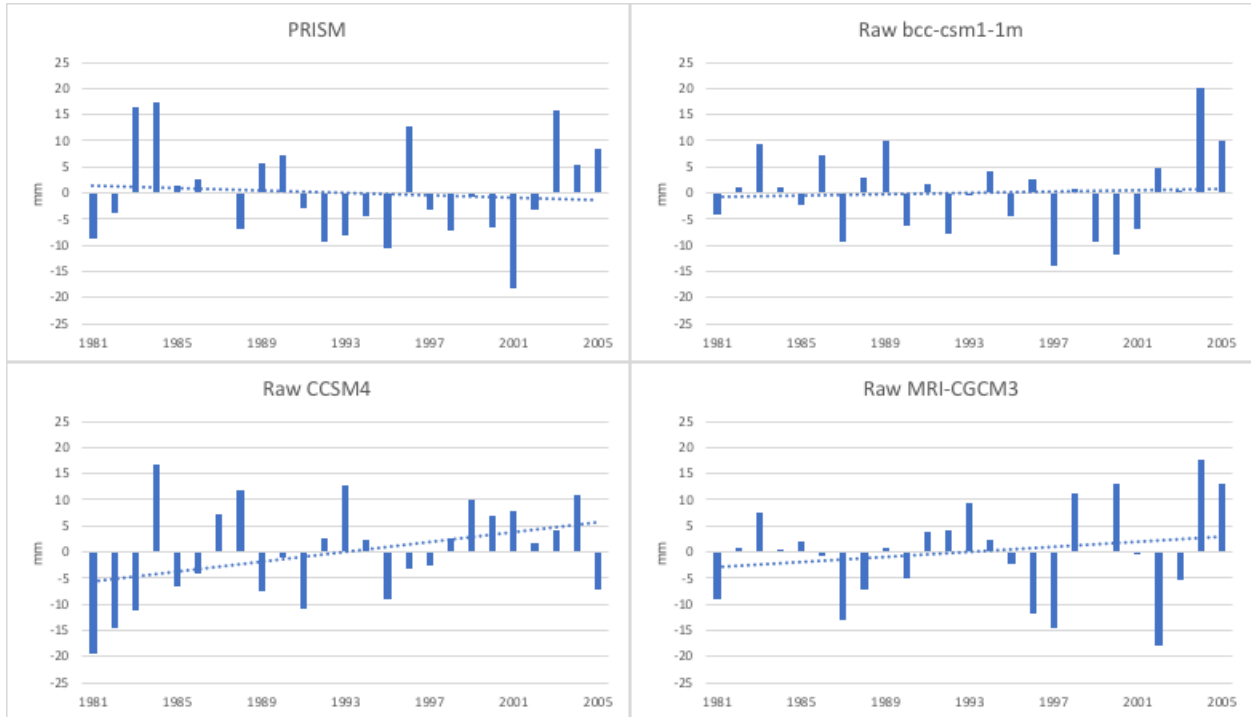


Figure 23- Anomalies for raw consecutive maximum 5-day precipitation

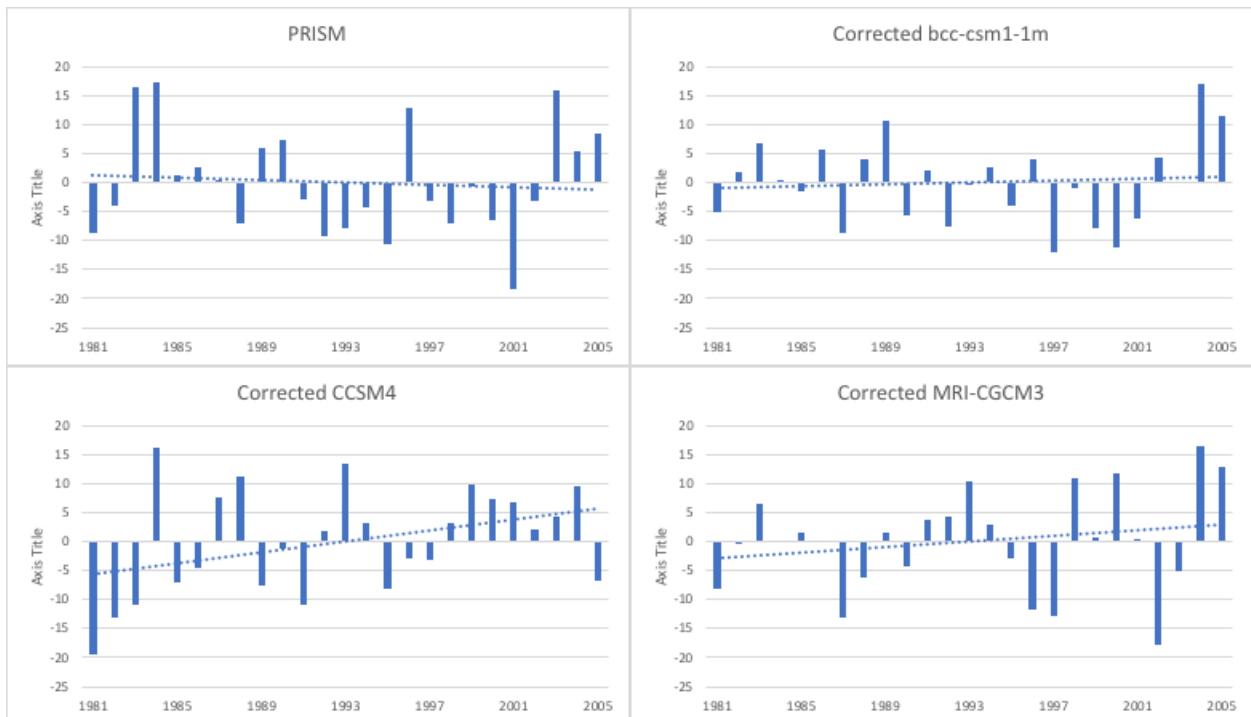


Figure 24 - Anomalies for bias-corrected consecutive maximum 5-day precipitation

Although bcc-csm1-1m and PRISM have a better correlation than those of PRISM against the other models, the trend lines show that PRISM, CCSM4, and MRI-CGCM3 all have positive trends in heavy precipitation (see Figure 25 and Figure 26). Bcc-csm1-1m is the only model with an overall negative trend.

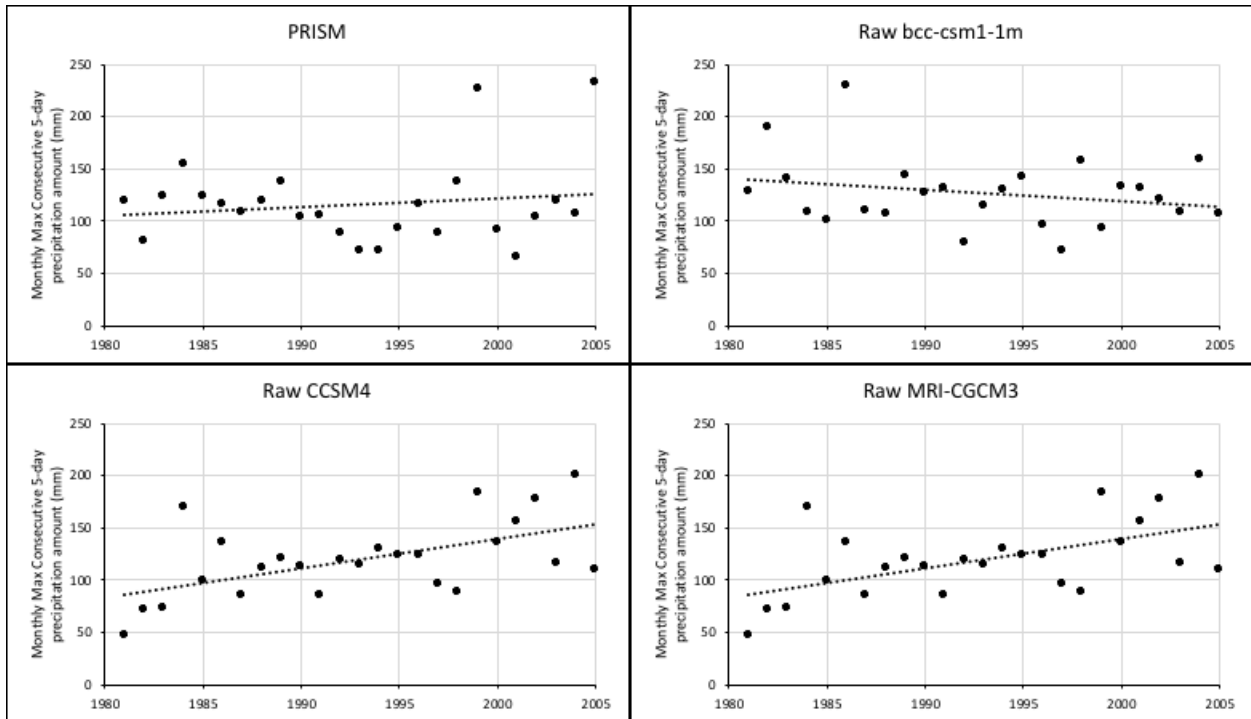


Figure 25 - Rx5day trends using raw data

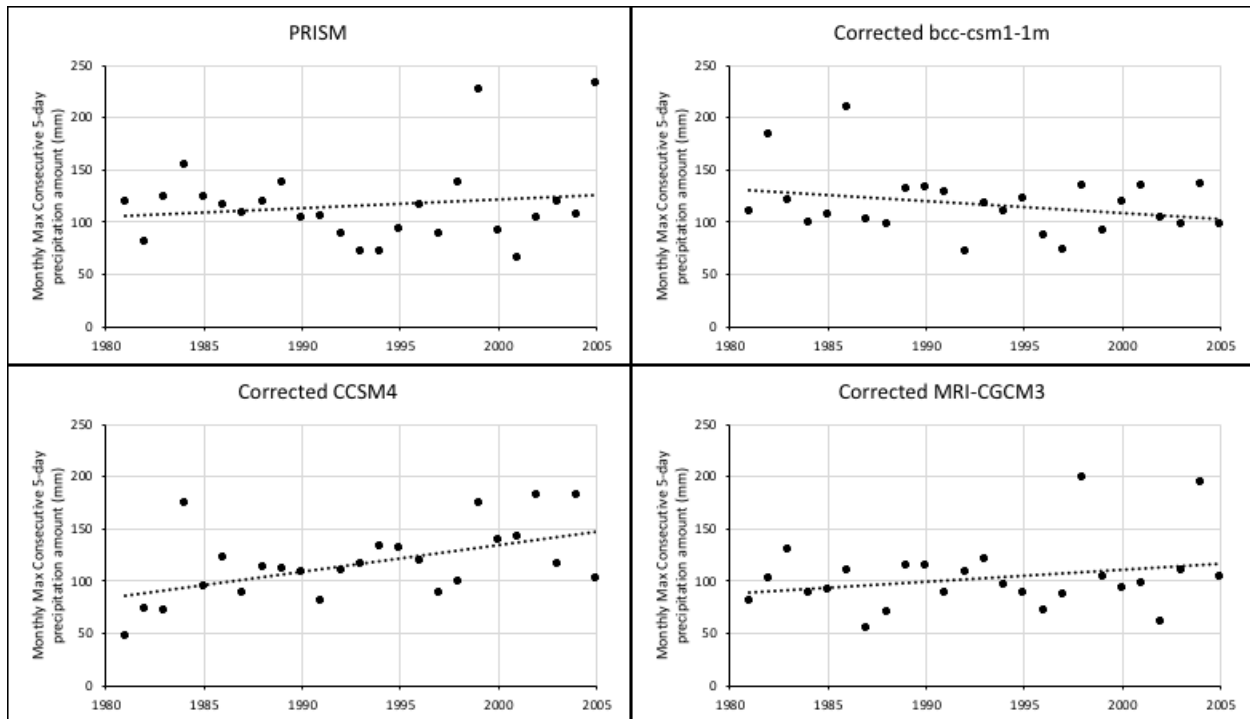


Figure 26 - Rx5day trends using corrected data

3.4 Future Changes in Extreme Climate Indices to the PRB

Having looked at the observed and the historical model output and validating the ability of the chosen models to provide reasonable data, future raw and corrected climate data were then run through RCLimDex in R to determine the potential changes in climate extremes under RCP 4.5 and RCP 8.5 for 2051-2075 relative to 1981-2005.

3.4.1 Temperature

3.4.1.1 TN10p

The models vary in output for the predicted cold nights. The models all agree that the amount of very cold nights will decrease, but at different rates dependent on the scenario used. These differences are shown very distinctly in Figure 27. CCSM4 and bcc-csm1-1m both agree that in scenario 4.5, there will be a decrease of about 0.1%, whereas scenario 4.5 for MRI-CGCM3 predicts a negative change of nearly 0.25%. Interestingly, both bcc-csm1-1m and MRI-CGCM3

both project that in RCP 8.5—the scenario in which emissions are widely unregulated—the TN10p will decrease to almost half of the respective predictions in RCP 4.5.

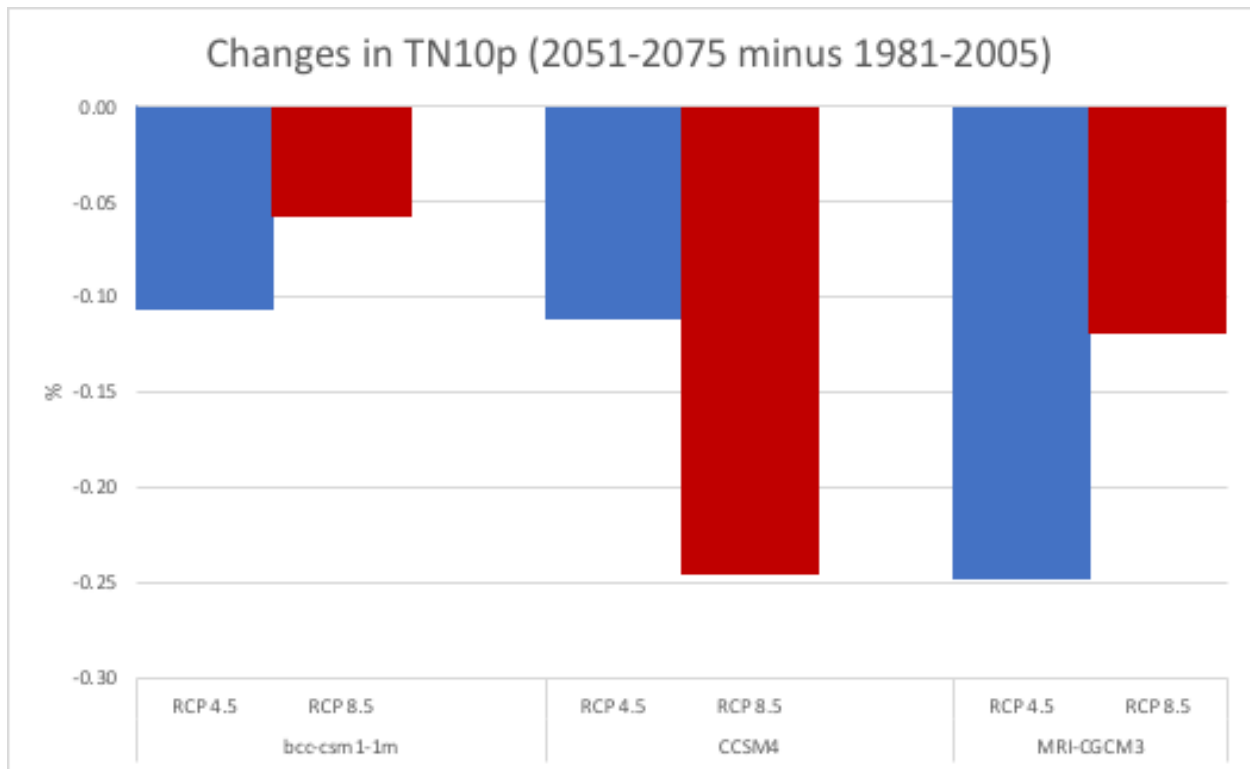


Figure 27 – Changes in TN10p

3.4.1.2 TN90p

The model output for change in TN90p is overall somewhat more in line with expectations for change in the PRB. Theoretically, RCP 8.5 should have a larger increase in the amount of warm nights; however, bcc-csm1-1m interestingly predicts that in both scenarios, there will be an approximate 0.25% increase in warm nights. CCSM4 presents an outlier and predicts that scenario 8.5 will have an overall decrease in warm nights. MRI-CGCM3 represents the expected outcome with RCP 8.5 showing a drastic increase in the warm nights over RCP 4.5. Despite the variations, 5 out of 6 future scenarios agree that there will be an increase in warm nights.

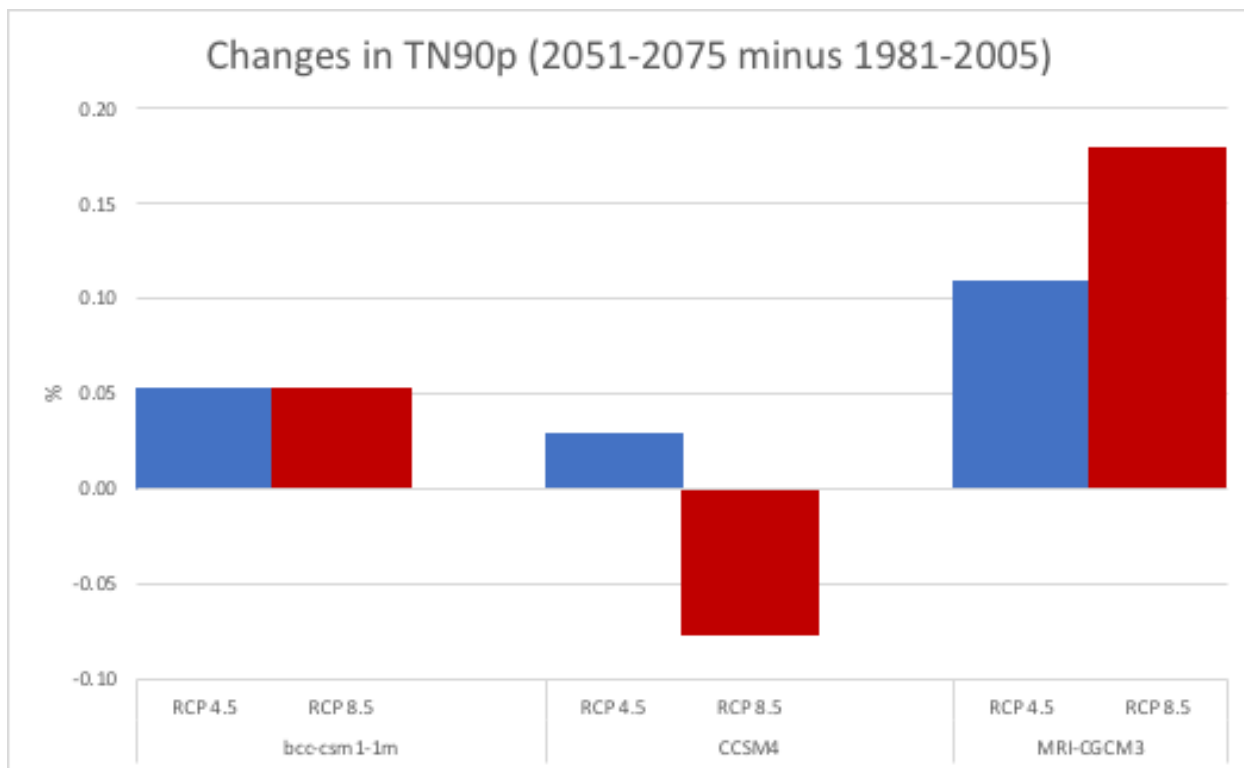


Figure 28 – Change in TN90p

3.4.2 Precipitation

3.4.2.1 CDD

Unsurprisingly, the distribution of consecutive dry days shows that the models predict varying outcomes for total change in CDD. Bcc-csm1-1m shows the 50th percentile between the scenarios remains approximately the same, with the upper quartile shifting higher for RCP 8.5 (see Figure 29 and Figure 30). The lower quartile also extends lower for scenario 8.5, so the total range of CDD is wider than the other scenarios. Bcc-csm1-1m is the only model that conforms to available literature that predicts that New Jersey and the mid-Atlantic states are predicted to see more frequent droughts despite heavier and more frequent precipitation. The other models show a decrease in CDD in comparison to their historical counterparts.

Corrections in precipitation data largely affect MRI-CGCM3, where both scenarios see shifts in their overall CDD. The corrected RCP 4.5 CDD 75th percentile decreases while the 50th percentile increases. For the corrected RCP 8.5 CDD, the median distributions equal out slightly.

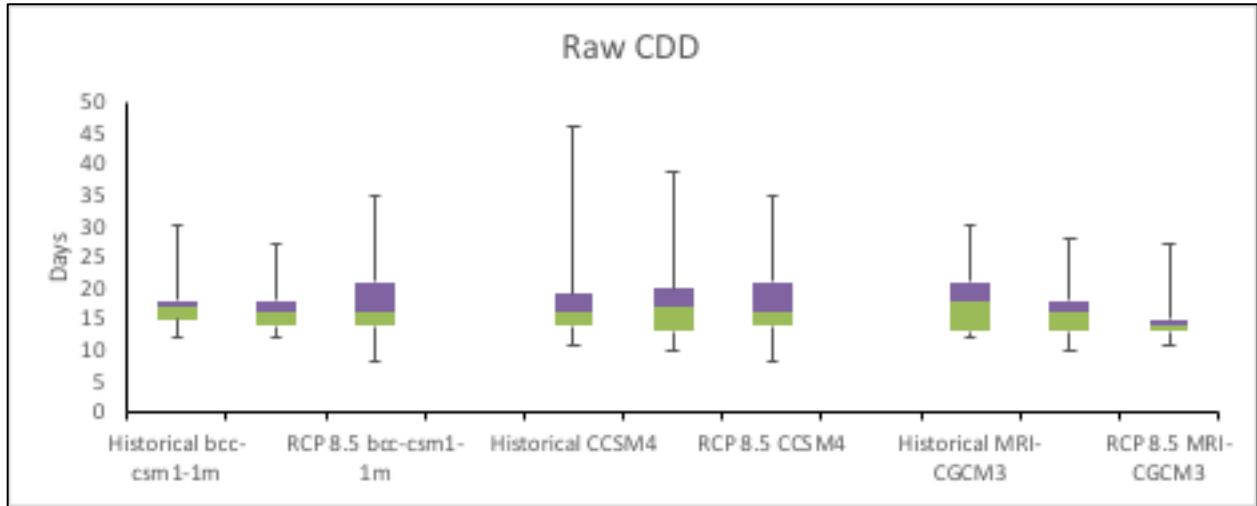


Figure 29 – Raw CDD for the three models in emissions scenarios 4.5 and 8.5

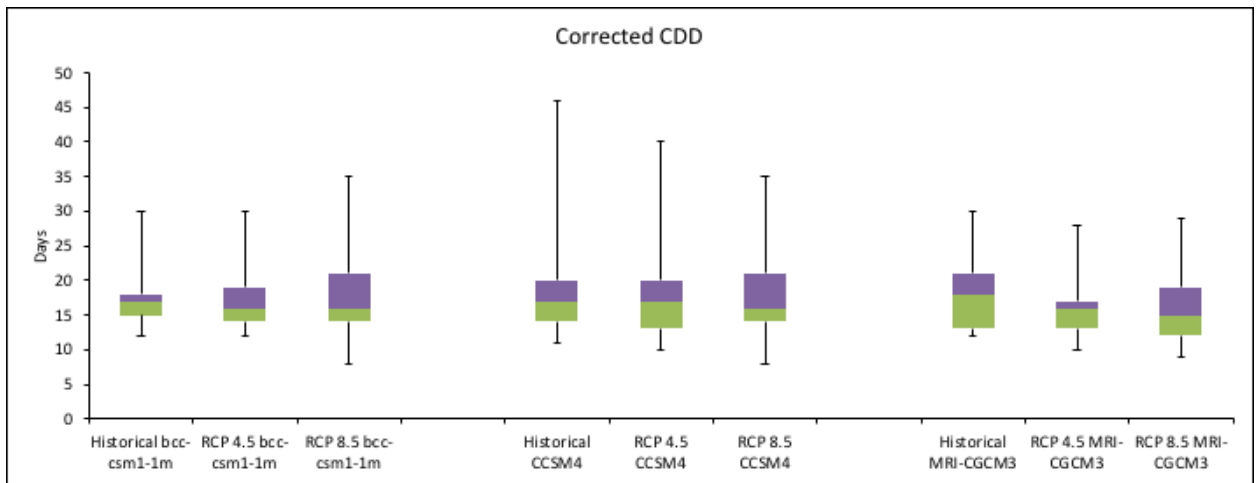


Figure 30 - Corrected CDD for the three models in emissions scenarios 4.5 and 8.5

While looking at the actual expected change between the average CDD relative to the historical CDD, MRI-CGCM3 and corrected CCSM4 show unexpected results (see Figure 31). MRI-CGCM3 shows an overall decrease in CDD in RCPs 4.5 and 8.5, whereas bcc-csm1-1m 8.5 shows an increase in overall consecutive dry days. Raw data from CCSM4 shows no change

between RCP 8.5 and the historical value for CDD, while the corrected version of the data shows a decrease in CDD.

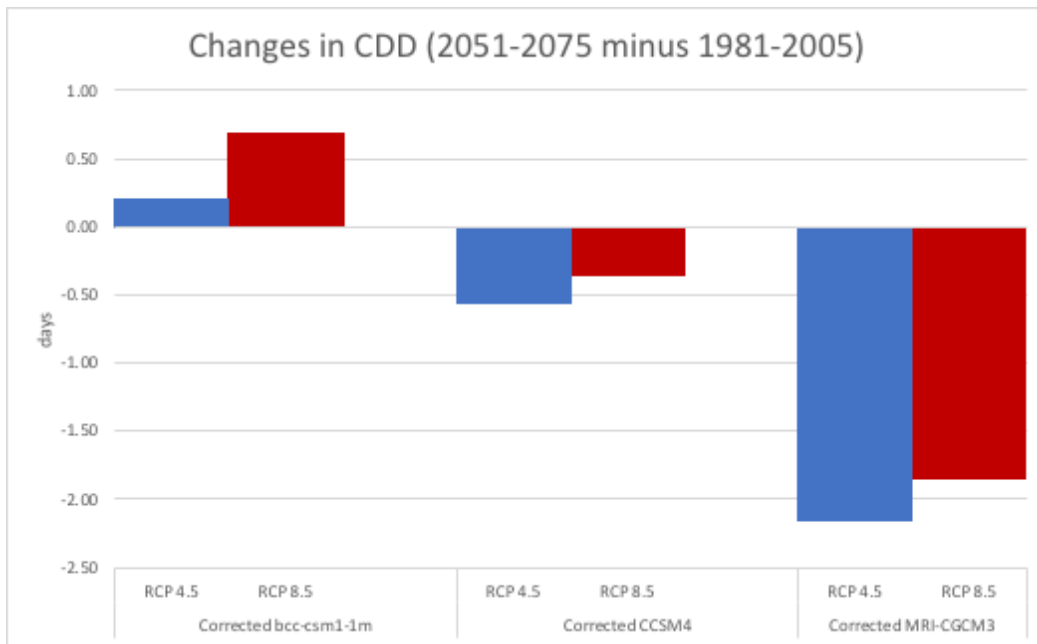


Figure 31 – Changes in CDD

3.4.2.2 R10

The differences in the distribution of days in which precipitation amounts to over 10 mm (R10) data between the 3 models do not drastically differ. CCSM4 shows that the 50th percentile of R10 days differs by approximately 2 days, but the maximum amount of days is approximately the same between the historic and future scenarios. Bcc-csm1-1m shows the most difference in distribution of data, with the full range of historic raw data extending from 30-55 days, RCP 4.5 ranging from 21-50 days, and RCP 8.5 ranging from 23-60 days. CCSM4 shows all climate scenarios with the same maximum value, while minimum values range from 22-26 and for 8.5 and 4.5 respectively. The lower and upper quartile of data from MRI-CGCM3 increase only slightly between the historic and emissions scenarios, with only the extremes shifting slightly. The corrected data distribution only slightly changes from the raw (see Figure 33).

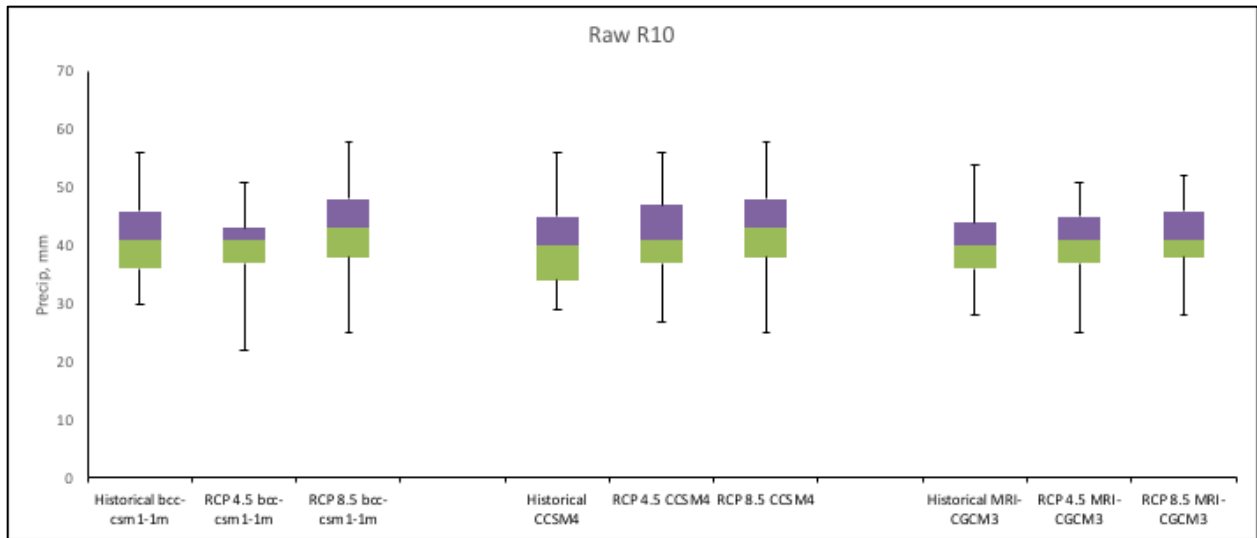


Figure 32 - Raw R10 for the three models in emissions scenarios 4.5 and 8.5

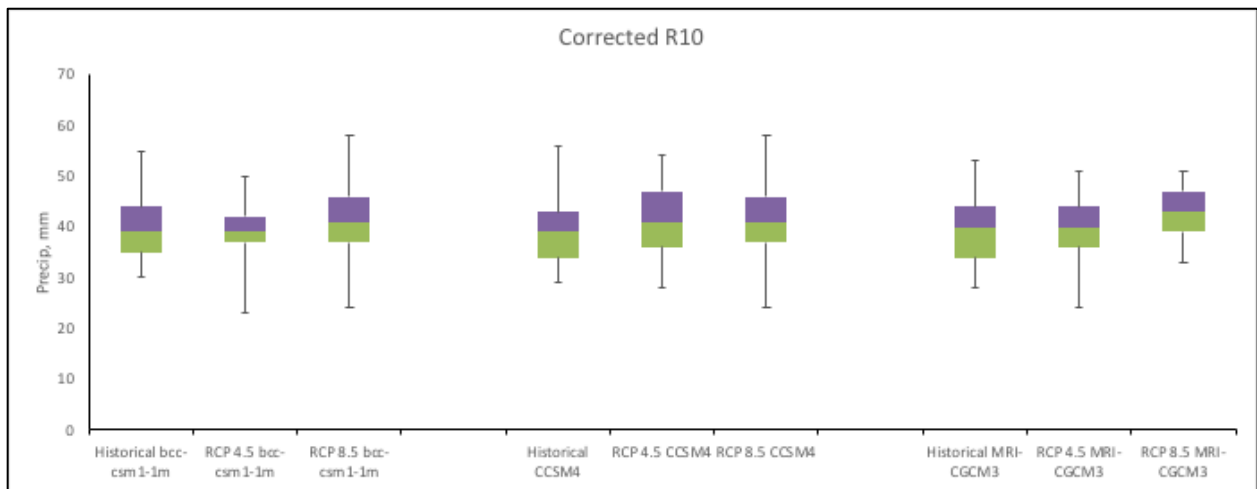


Figure 33 – Corrected R10 for the three models in emissions scenarios 4.5 and 8.5

Examining the total change between the future average compared to the historical average R10, the models agree that there is an expected increase in total days in which the precipitation falls over 10 mm in RCP 8.5 (see Figure 34). However, RCP 4.5 has mixed output. Bcc-csm1-1m shows a decrease in precipitation in comparison to the baseline time period for RCP 4.5, CCSM4 shows an increase of only 1-1.5 days, and MRI-CGCM3 shows a decrease for the raw data and an increase for the corrected data.

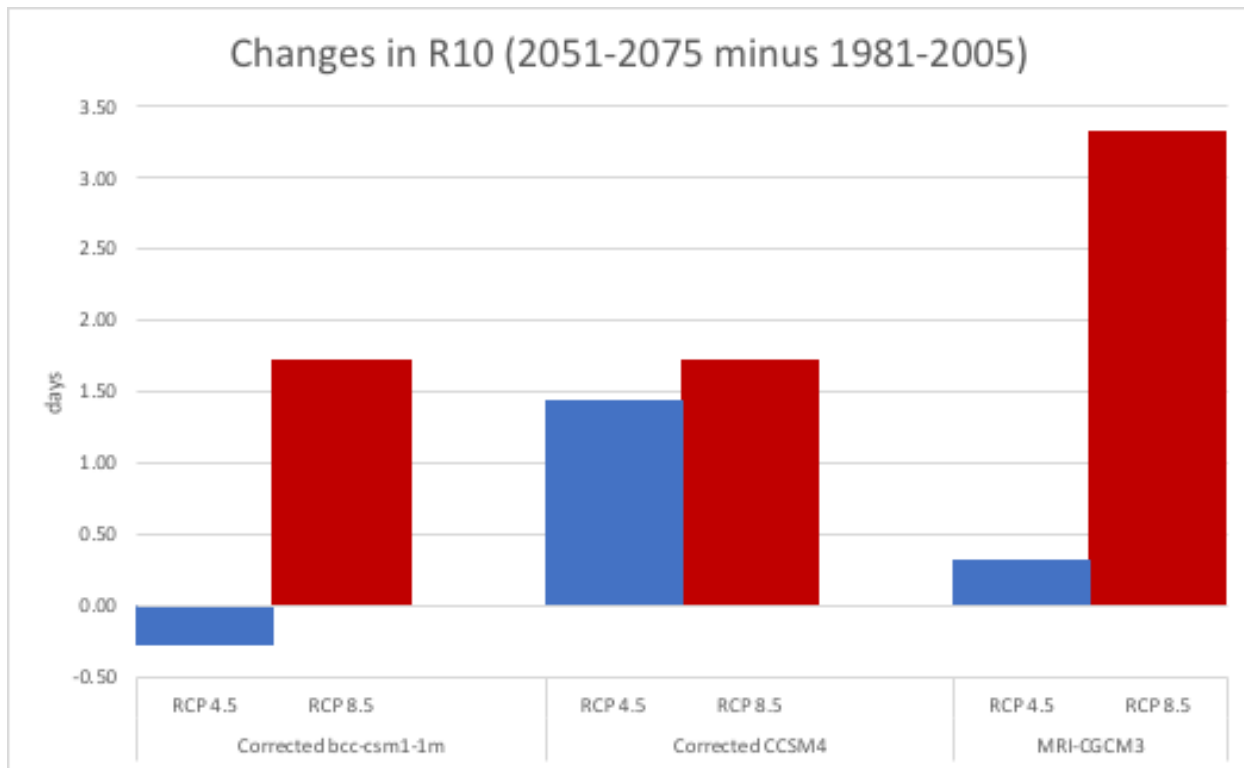


Figure 34 – Change between future average R10 relative to average historical R10

The historic plots in Figure 35 show average precipitation amounts for the winter and summer months. Though there are differences between the models, with the overestimation of bcc-csm1-1m summer precipitation clear, most of the PRB (outlined in red) shows summer precipitation to fall between 3-5 mm.

Winter months show average precipitation to historically be between 2 and 4 mm. However, when looking at the average expected R10 from RCP 8.5, the models heavily disagree (see Figure 36). Bcc-csm1-1m shows the full range of values available, while MRI-CGCM3 is only slightly more varied, with a range from 10-70 days per year.

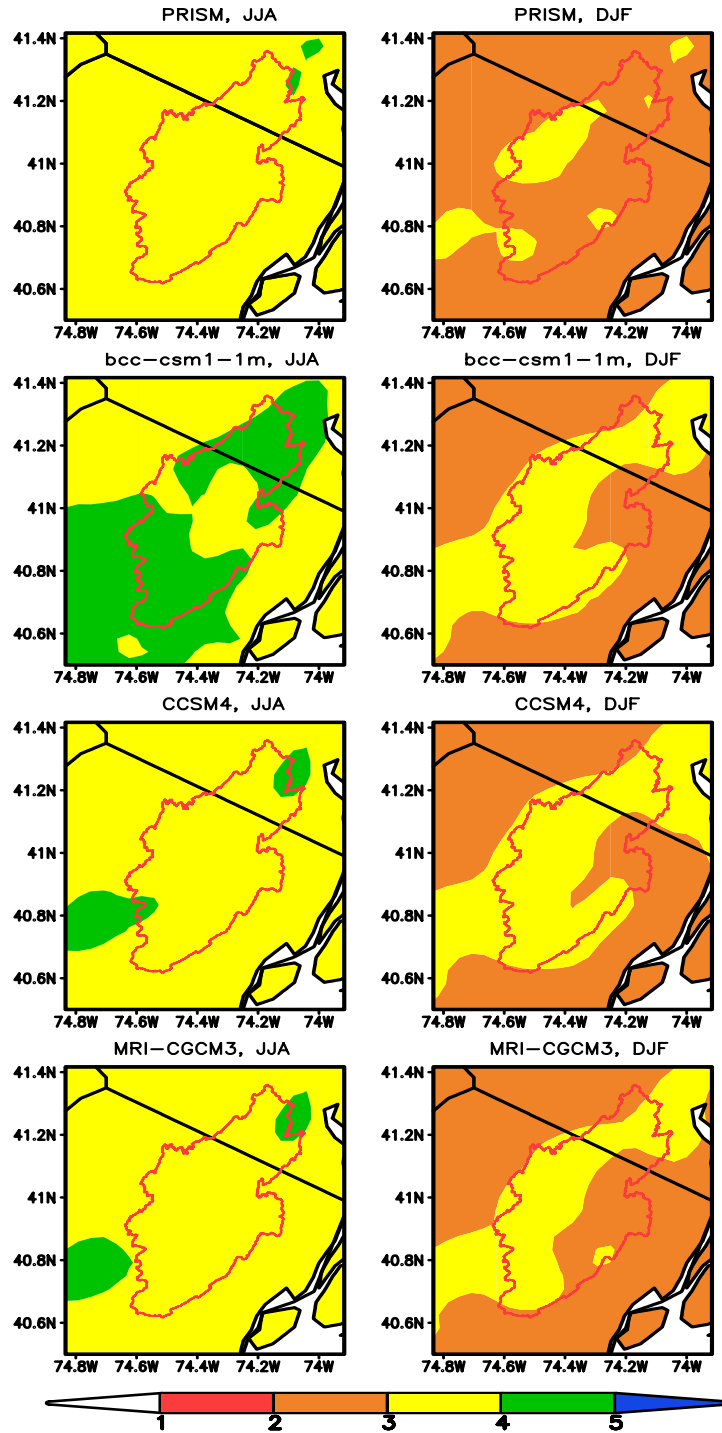


Figure 35 – Average historical (1981-2005) summer and winter precipitation (mm) from observed (PRISM) and MACA models. The orange areas represent precipitation amounts ranging from 2-3 mm; yellow areas represent precipitation amounts ranging from 3-4 mm; the green areas represent precipitation amounts ranging from 4-5 mm.

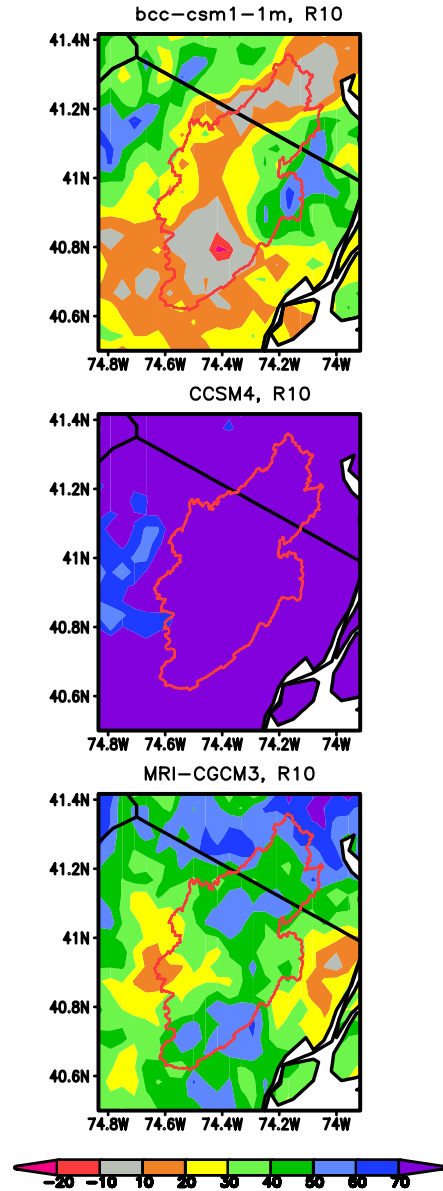


Figure 36 - Projected changes in heavy wet-weather days in which precipitation is greater than 10 mm (R10) in RCP 8.5

CCSM4, on the other hand, shows the whole PRB to experience more than 70 days in which precipitation is greater than 10 mm.

3.4.2.3 R95p

The expected change between the historic average R95p and the historic R95p is relatively united amongst the models. In RCP 8.5, each of the models anticipate a minimum of 30 mm of intense precipitation, with a maximum of nearly 80 mm. RCP 4.5 sees a slightly more varied

distribution of data, but all models except MRI-CGCM3 see an increase in average R95p. In most of these climate scenarios, the amount of intense precipitation will increase significantly (see Figure 37).

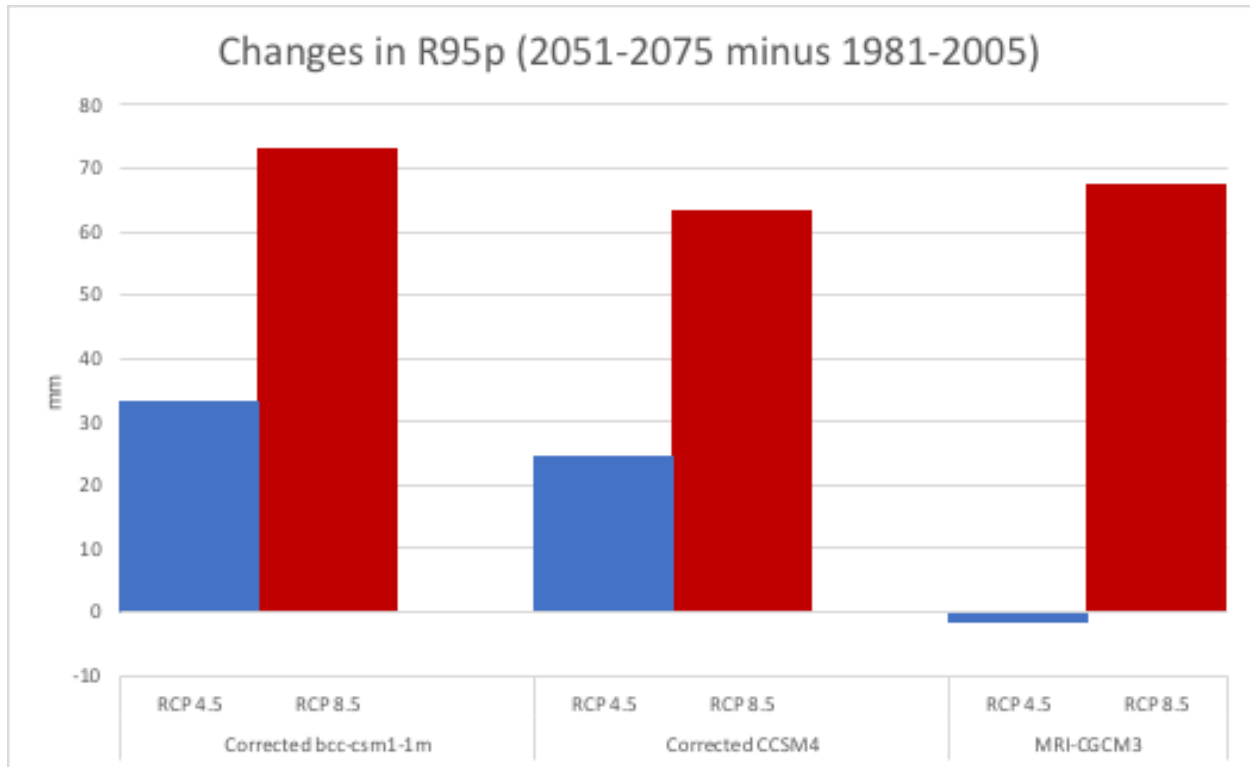


Figure 37 – Changes in R95p

3.4.4.4 Rx5day

The monthly maximum 5-day precipitation addresses the frequency of precipitation whereas the other climate indices related to precipitation address the absence of precipitation or the amount. The models agree in RCP 8.5 that the maximum 5-day precipitation amount will increase, with values of precipitation ranging from 20 mm to approximately 48 mm. As with the R95p, bcc-csm1-1m and CCSM4 also agree—albeit bcc-csm1-1m predicts nearly 4 times the intensity of CCSM4—that the Rx5day will increase in scenario 4.5, while MRI-CGCM3 predicts decreases in the frequency of consecutive rainy days.

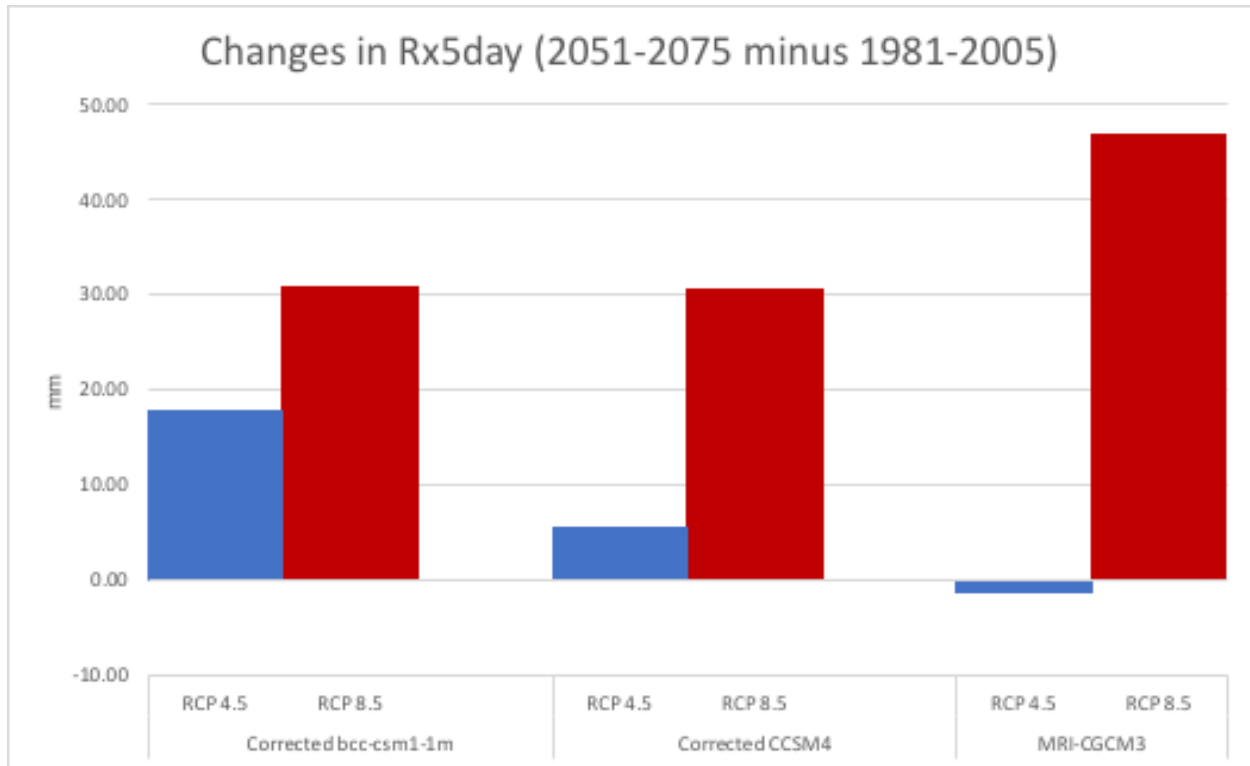


Figure 38 – Changes in Rx5day

Plotting seasonal changes over the PRB provides more in-depth analysis. Figure 39 shows that plotting the average Rx5day provides further insight to the expected changes in the PRB for scenario RCP 8.5. Bcc-csm1-1m shows a gradient of change with average precipitation decreasing by 10 towards the east. All the models seem to agree that the areas further east will experience lower extreme rainfall than the western regions. Bcc-csm1-1m and MRI-CGCM3 both expect the easternmost regions along the border of the PRB will experience less amounts of total average precipitation in the 2051-2075. These two models also show no total increase or decrease in parts of the eastern half of the PRB. CCSM4, on the other hand, shows a total average increase of approximately 120 mm over the basin area.

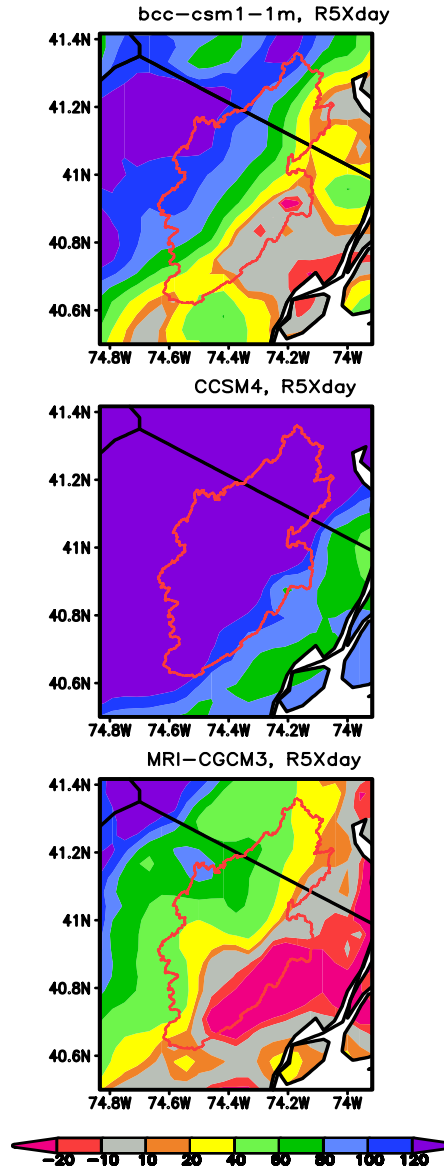


Figure 39 – Projected trends of maximum consecutive 5-day precipitation in emissions scenario RCP 8.5

4. Discussion

While performing bias-correction of the precipitation data, we found that MACA simulations improved better with the linear correction factor than the more sophisticated quantile mapping. The interpretation of the CDF graphs showed a significant difference between the two methods and therefore the correction factor method was a preferred method of validation. MACA is not a hindcasting RCM; therefore, although the daily correlations were still insignificant,

seasonal statistical analysis showed significantly improved accuracy. Because of this improvement, we believe that MACA sufficed for longer time scales and gave us confidence in MACA's ability to diagnose long-term climate extremes. This validation of the simulated climate for the baseline 1981-2005 time period allowed for bias-correction for the future projections for 2051-2075.

While looking at the results for the climatic extremes, we expected precipitation and temperature extreme indices calculated amongst the models to universally agree that RCP 4.5 would show less extreme results while RCP 8.5 would show more dramatic differences. However, our initial hypotheses were proven false. For the 10th percentile of cold nights, the models agree that there will be less extremely cold days, but RCP 8.5 for bcc-csm1-1m and MRI-CGCM3 shows less of a decrease than RCP 4.5. The models generally also see an increase in the days per year that will experience warmer nights, except in the case of CCSM4 RCP 8.5, which sees a decrease in the 90th percentile of warm nights. Given that there is an overall increase in wet days, extreme precipitation, and consecutive precipitation, we hypothesize that this impact on temperature is perhaps due to increased precipitation and associated cloudiness. The increase of rainfall seen by decreased consecutive dry days and the other extreme precipitation indices is most likely due to decreased longwave cooling at nights—therefore, there would be a reduced amount of very cool nights and an increase in warm nights.

This study heavily emphasizes the importance of using downscaled GCM climate data to determine the potential impacts of climate change on localities. Figures 36 and 39 both emphasize the potential differences in climate extremes for the PRB. Visualizing the differences in wet days and the differences in heavy precipitation amounts is helpful in delivering detailed climate change analysis. The rainy days are heavily varied within the boundary of the PRB; bcc-csm1-1m shows

changes ranging from a decrease of 20 days to an increase of 60-70 days, CCSM4 sees an increase 70 days for the whole basin, while MRI-CGCM3 sees an increase of anywhere from 10 to 70 days. The usefulness of using an RCM can be seen again with the range of differences in the consecutive wet days—the differences amongst the areas in the PRB are defined and clear. Bcc-csm1-m and MRI-CGCM3 see that there is a decrease in the amount of rain the further east you go whereas CCSM4 overall just sees an increase of 130 mm. These differences would not be possible to map without downscaling and bias correcting GCM data.

Knowing the trend for cold nights can also be helpful for healthcare professionals, urban planners, industry, the vulnerable populations, and other involved stakeholders. The increase in amount and frequency of wet days and can be especially helpful for urban planners who need to know how to design adaptable infrastructure to protect against flooding, growth of invasive species, or other prospective infrastructure failures. Knowing about the potential increase in very warm nights can also be particularly helpful for those in the healthcare industry, who can advise the general population about issues such as spreading diseases from ticks, mosquitoes, and other similar disease-carrying insects. Being armed with this information can also be incredibly helpful for the vulnerable populations, such as the very young, very old, homeless, or those in urban areas without access to cooling.

Future work can extend in different directions. Firstly, incorporating more of the 20 available downscaled, bias-corrected MACA models would help create a fuller, more comprehensive understanding of the potential impacts of climate change on the PRB. A sustainability assessment could also be done with the data to help ensure that as the PRB experiences changes, the population experiences socially equitable, economically sustainable, and environmentally sound decision making to increase community resilience. Urban planners and

engineers could also use the available projections to incorporate green infrastructure to their plans, creating a more sustainable PRB. Ultimately, downscaled, bias-corrected GCM data can prove to be very helpful for smaller regions.

5. Potential Sources of Error

There may have been several sources of error in the MACA dataset. The developers of MACA note potential uncertainty arising from climate sensitivity and difficulty in incorporating unpredictable human and political actions into the model. GCMs themselves also have difficulty making predictions for smaller-level storm fronts. There is also concern that the model does not take the impact of the heat island effect into account; therefore, the model may show better results in more vegetated areas rather than heavily industrialized areas such as New Jersey.

6. Conclusion

The purpose of this study is to identify the ways in which climate change would affect the Passaic River basin by using the MACA model. Many regional climate models (RCMs) like MACA take information from Global Climate models and downscale and bias-correct the data through their own algorithms. When we bias-corrected the data against another model, using PRISM as the observational dataset, the correlations did not significantly improve the correlation coefficient for either precipitation or temperature. When the linear method of using a correction factor did not drastically improve the correlation, R^2 , and RMSE, a more sophisticated approach of correction was implemented, in which quantile mapping transformed the MACA data. However, while analyzing the CDFs from the raw, linear corrected, and quantile mapped MACA data, the CDF of the quantile-mapping corrected data significantly differed from that of the observed dataset. Because the cumulative distribution of the raw and corrected data so closely matched the observed distribution, it was considered a reasonable dataset to use to determine assess future

changes in climate extremes. For temperature, bias-correction sometimes actually made the correlation coefficient worse and therefore, further temperature bias-correction beyond the MACA-implemented measures were not performed. Ultimately, MACA downscaled and bias-corrected CMIP5 climate projections seem to suffice for detailed analysis of climate impacts at monthly or longer time periods.

Using the data to analyze future climatology patterns provided interesting results. The disagreement between the models for the different radiative forcing scenarios was surprising. The changes in extremes were not always larger for stronger radiative forcing changes. The decrease in climate extremes for RCP 8.5 is most probably due to the increase in cloudiness from the projected increases in amount and frequency of precipitation. The increase in both precipitation days over 10 mm and the annual precipitation days in which the precipitation exceeded the 95th percentile was expected given the expectations for New Jersey as a whole to experience higher amounts of precipitation (EPA, 2016). While the results from the models analyzed vary considerably, this study underscores the usefulness of employing downscaled and bias corrected climate projections for investigating plausible future changes at the basin scale.

Scientifically sound information concerning information on climate extremes is of great value for formulating policies to adapt to the change in climate. Policies can be implemented at local level to help improve community resilience. Urban planners as well as agricultural and healthcare professionals can benefit from credible projections in changes in climate extremes.

References

- Abatzoglou, J., 2013. *MACA Methods - Steps*. [Online]
Available at: <https://climate.northwestknowledge.net/MACA/MACAMethod.php>
- Camici, S., Brocca, L., Melone, F. & Moramarco, T., 2014. Impact of Climate Change on Flood Frequency Using Different Climate Models and Downscaling Approaches. *Journal of Hydrologic Engineering*, 19(8), pp. 04014001-15.
- Chen, J., Brissette, F. P., Chaumont, D. & Braun, M., 2013. Finding appropriate bias correction methods in downscaling precipitation for hydrologic impact studies over North America. *Water Resources Research: An AGU Journal*, 49(7), pp. 4187-4205.
- ClimDEX, 2013. *Climate Extremes Indices*. [Online]
Available at: <https://climdex.org/indices.html>
- Daly, C. & Bryant, K., 2013. *The PRISM Climate and Weather System – An Introduction*. [Online]
Available at: http://www.prism.oregonstate.edu/documents/PRISM_history_jun2013.pdf
[Accessed 5 June 2018].
- Daly, C. et al., 2017. High-resolution precipitation mapping in a mountainous watershed: ground truth for evaluating uncertainty in a national precipitation dataset. *International Journal of Climatology*, 37(1), pp. 124-137.
- Data Camp, 2016. *Python tutorial: Cumulative Distribution Functions*. [Online]
Available at: <https://www.youtube.com/watch?v=ap4mfGvgDsM&t=101s>
- Demirel, M. C. & Moradkhani, H., 2015. Assessing the impact of CMIP5 climate multi-modeling on estimating the precipitation seasonality and timing. *Springer Science*, 14 November, pp. 357-372.
- Demirel, M. C. & Moradkhani, H., 2016. Assessing the impact of CMIP5 climate multi-modeling on estimating the precipitation seasonality and timing. *Climate Change*, Volume 135, pp. 357-372.
- Environmental Protection Agency, 2012. *Reducing Urban Heat Islands: Compendium of Strategies, Cool Pavements*. [Online]
Available at: https://www.epa.gov/sites/production/files/2017-05/documents/reducing_urban_heat_islands_ch_5.pdf
- Environmental Protection Agency, 2017. *Heat Islands*. [Online]
Available at: <https://www.epa.gov/heat-islands/learn-about-heat-islands>
- EPA, 2016. *What Climate Change Means for New Jersey*. [Online]
Available at: <https://19january2017snapshot.epa.gov/sites/production/files/2016-09/documents/climate-change-nj.pdf>
[Accessed 9 March 2018].
- Eum, H.-I., Cannon, A. J. & Murdock, T. Q., 2017. Intercomparison of multiple statistical downscaling methods: multi-criteria model selection for South Korea. *Stochastic Environmental Res Risk Assessment*, Volume 31, pp. 683-703.
- Gudmundsson, L., 2016. *qmap: Statistical Transformations for Post-Processing Climate Model Output*. [Online]
Available at: <https://rdrr.io/cran/qmap/>
- Hempel, S. et al., 2013. A trend-preserving bias correction – the ISI-MIP approach. *Earth System Dynamics*, Volume 4, pp. 219-236.

IPCC , 2013. *Climate change 2013: the physical science basis*, Cambridge: Cambridge University Press.

IPCC Climate Report, 2007. *TOWARDS NEW SCENARIOS FOR ANALYSIS OF EMISSIONS, CLIMATE CHANGE, IMPACTS, AND RESPONSE STRATEGIES*. [Online]
Available at: <http://www.aimes.ucar.edu/docs/IPCC.meetingreport.final.pdf>

Kümmel, H., 1895. *Lake Passaic: An Extinct Glacial Lake*. Trenton: John L. Murphy Publishing Company .

Karl, T. R., Melillo, J. M. & Peterson, T. C., 2009. *Global Climate Change Impacts in the United States*, s.l.: Cambridge University Press.

Kim, J. et al., 2017. Winter precipitation characteristic in western US related to atmospheric river landfalls: observations and model evaluations. *Climate Dynamics*, Volume 50, pp. 231-248.

Kim, M.-K. et al., 2016. Statistical downscaling for daily precipitation in Korean using combined PRISM, RCM, and quantile mapping: part 1, methodology and evaluation in historical simulation. *Journal of Atmospheric Science*, 7 March, 52(2), pp. 79-89.

MACA, 2013. *MACA Home*. [Online]
Available at: <http://maca.northwestknowledge.net/MACAanalysis.php>

MACA, 2013. *MACA Training Data*. [Online]
Available at: <https://climate.northwestknowledge.net/MACA/MACATrainingdata.php>

Mote, P., Rupp, D. & Abatzoglou, J., 2015. *Evaluation and downscaling of CMIP5 climate simulations for the Southeast US*, s.l.: Oregon State University and University of Idaho.

Mote, P., Rupp, D. & Abatzoglou, J., 2015. *Evaluation and downscaling of CMIP5 climate simulations for the Southeast US*, s.l.: U.S. Geological Survey.

NASA, 2018. *The consequences of climate change*. [Online]
Available at: <https://climate.nasa.gov/effects/>

National Center for Atmospheric Research, 2018. *What is Downscaling?*. [Online]
Available at: <https://gisclimatechange.ucar.edu/question/63>

NJ Highlands Coalition, n.d. *The Region*. [Online]
Available at: <http://njhighlandscoalition.org/the-region/>

NOAA, 2016. *Historic Crests*. [Online]
Available at:
http://water.weather.gov/ahps2/crests.php?wfo=phi&gage=ltn4&crest_type=historic
[Accessed 9 March 2018].

PRISM, 2016. *Descriptions of PRISM Spatial Climate Datasets for the Conterminous United States*. [Online]
Available at: http://www.prism.oregonstate.edu/documents/PRISM_datasets.pdf
[Accessed 5 June 2018].

Rupp, D. E., Abatzoglou, J. T., Hegewisch, K. C. & Mote, P. W., 2013. Evaluation of CMIP5 20th century climate simulations for the Pacific Northwest USA. *Journal of Geophysical Research*, 118(19), pp. 10884-10906.

Thibeault, J. M. & Seth, A., 2014. Changing climate extremes in the Northeast United States: observations and projections from CMIP5. *Climatic Change*, Volume 127, pp. 273-287.